NTNU – Trondheim
Norwegian University of
Science and Technology

Spin-Polarized Non-Local Transport in Hybrid Structures with Magnetic and Superconducting Correlations

Kristoffer Stige

Master of Science in Physics and Mathematics
Submission date: May 2012
Supervisor: Jacob Rune Wüsthoff Linder, IFY

Norwegian University of Science and Technology
Department of Physics

Abstract

In this thesis we theoretically examine spin-polarized non-local transport in two junctions built up by materials with superconducting and magnetic properties. The first consists of a Zeeman-split superconductor placed between two normal metals. We find that such systems can generate a spin-polarized non-local current even when the injected current is unpolarized. The effect is however mostly geometric and take place also when the superconductor is switched with a normal metal. The second system is built up by two ferromagnetic wires coupled by a superconductor via spin-active interfaces. We investigate the circumstances which allow for an inverse spin-valve effect. For certain parameter ranges we find that a crossover between positive and negative magnetoresistance is possible as a function of temperature.

Acknowledgements

I would like to thank my supervisor Jacob Linder at the Department of Physics, NTNU, who has offered valuable assistance and guidance during my work with this Master thesis.

I am very grateful to my family, especially to my parents, for their care and support. Without mentioning names, I would also like to thank all of my friends for showing interest in my work.

Above all, I want to express my deepest thanks to my Saviour with the words of Ephesians 1,3-14.

Contents

Chapter 1

Introduction

Superconductivity is the complete disappearance of electrical resistivity and expulsion of the magnetic field at temperatures below a material-dependent critical temperature. The current in conventional superconductors is carried by a condensate of Cooper pairs, consisting of two electrons at the Fermi level with opposite spins and zero center of mass momentum. This condensate is seperated from the one-particle states of the superconductor by the superconducting gap Δ. To break a pair and create particle excitations above the condensate an energy of at least 2Δ is required.

Superconductivity was discovered hundred years ago in 1911. Since then many theoretical and experimental studies have been performed to investigate this special property. For some years superconducting hybrid structures have got a lot of attention. Systems built up by layers of normal metals and superconductors show interesting transport properties, and can lead current also when the energy of the incoming particles are below the superconducting gap energy.

Since the 1990s spintronics has been a growing field of research. Spintronics combine the two fundamental properties of the electron, namely charge and spin. One thus looks at the combined effect of electronics and magnetism. Usually this is based on ferromagnetic materials, which to some extent can give spin-polarized currents. A spintronic device is strongly dependent of the degree of spin polarization in the current and the performance improves for increasing polarization. Therfore one of the main research activities in spintronics is how to obtain and manipulate spin-polarized currents.

A recent idea is to combine superconducting properties with spin manipulation. This subfield of spintronics is by some called superspintronics. In the most usual form of superconductors the Cooper pairs have antiparallel spins and thus have a total spin of zero, and the superconductor is said to have a spin-singlet symmetry. A magnetic field will try to align the spins with the field. Magnetism and superconductivity are thus opposing effects in the normal case. However, as we see in chapter 3 magnetic and superconducting properties can correlate under certain conditions. Another option that will not be given much space in this thesis are the so called spin-triplet

superconductors that can have parallel spin alignment of Cooper pairs.

This thesis will consentrate on two specific systems coupling magnetic and superconducting properties. The first system is motivated by a paper [1] that theoretically investigates a hybrid structure built up by a Zeeman split superconductor in contact with a normal metal. Zeeman split superconductors offer a synthesis between magnetic and superconducting correlations coexisting in the same material. They find the possibility to obtain a strongly polarized current in that system. We will look at a system where the Zeeman split superconductor is placed between two normal metals. As far as we know the spin properties of this system has not previously been studied in the literature. Since the density of states in the superconductor in this case will be spin-dependent we may look at processes such as spin-polarized crossed Andreev reflection. Of special interest is it to investigate if an injected unpolarized current could give rise to a spin-polarized non-local current, and which conditions that would have to be fulfilled.

The second system is also a novel system in the literature. It consists of a superconductor placed between two ferromagnets, where the barrier potentials at each interface is spin-dependent. A recent experiment [2] has indicated that such a sytem can give a transition between positive and negative magnetoresistance as a function of temperature and of barrier strength. We want to give this a thorough and systematic investigation to find what criteria must be fulfilled for this to happen.

This thesis is organized as follows. Chapter 2 will give a short introduction to superconductors and processes taking place in superconducting hybrid structures. In chapter 3 we will take a look at how superconducting and magnetic properties can coexist. The N-ZS-N system will be the focus of chapter 4 while the F-S-F system with spin-dependent interface potentials is investigated in chapter 5. Finally a conclusion is given in chapter 6.

The reader is assusmed to have some knowledge in the subject of quantum theory of solid matters. Readers familiar with superconductors and the correlations between superconducting and magnetic properties may skip ahead to chapter 4. Vectors will be given in bold-face notation, e.g. $\mathbf{k}$. Throughout most of the text we will use the convention $\hbar = 1$.

Chapter 2

Superconductors

This chapter will give a brief review of the theory for describing superconductors. In the coming chapters we are going to use this to find the wave functions and excitation energies of systems where correlations between superconducting and magnetic properties are present. Since many of the same transport processes are present in different hybrid structures with superconducting layers, we will briefly explain the concept behind these processes.

2.1 BCS-theory

The BCS-theory is a theory describing the properties of superconductors on a microscopic level. It was introduced by Bardeen, Cooper and Schrieffer in 1957 [3, 4]. They used quantum theory to investigate the coupling between electrons and phonons which is essential to understand superconductors. An incoming electron that collides with an ion causes a temporarily dipole moment around the lattice point. A second electron can be attracted by this dipole moment if the first electron has moved so far that the Coulomb repulsion between them is weaker than the attraction. We thus have a phonon mediated attractive interaction (see Fig. 2.1). This is possible if the two electrons are close to the Fermi surface and on the opposite sides of it, that means electrons with momenta $\mathbf{k}$ and $-\mathbf{k}$. Such pairs of electrons are called Cooper pairs [5], and the BCS-theory explains superconductivity as a condensation of such pairs into a superconducting condensate.

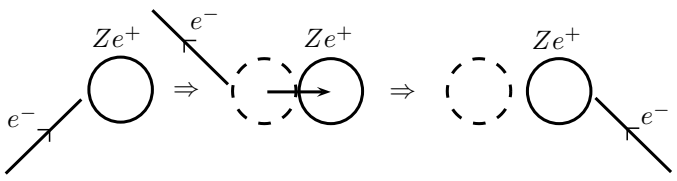

Figure 2.1: Classical picture of the phonon mediated attractive interaction between two electrons. This interaction was the first interaction used to describe superconductivity.

Based on this a Hamiltonian for superconductors can be derived. It is named the BCS-Hamiltonian and in second quantized form it can be written as:

$$H = \sum_{\mathbf{k},\sigma} \varepsilon_{\mathbf{k}} c^{\dagger}_{\mathbf{k}\sigma} c_{\mathbf{k}\sigma} + \sum_{\mathbf{k},\mathbf{k}'} V_{\mathbf{k}\mathbf{k}'} c^{\dagger}_{\mathbf{k}\uparrow} c^{\dagger}_{-\mathbf{k}\downarrow} c_{-\mathbf{k}'\downarrow} c_{\mathbf{k}'\uparrow} \tag{2.1}$$

where $\varepsilon_{\mathbf{k}}$ and $\mathbf{k}$ are the electrons kinetic energy and momentum respectively. $\uparrow$ and $\downarrow$ represents spin up and spin down. $V_{\mathbf{k}\mathbf{k}'}$ is the two-electron effective interaction (not specified at this point). $c^{\dagger}_{\mathbf{k}\sigma}$ and $c_{\mathbf{k}\sigma}$ are Fermi creation and annihilation operators fulfilling the usual anticommutator relations $\left\{c_{\mathbf{k}\sigma}, c^{\dagger}_{\mathbf{k}'\sigma'}\right\} = \delta_{\mathbf{k},\mathbf{k}'}\delta_{\sigma,\sigma'}$, with all other anticommutators equal to zero.

By using a mean-field approximation and introducing a new fermion basis we can write

$$H = H_0 + \sum_{\mathbf{k}} E_{\mathbf{k}} \left(\gamma^{\dagger}_{\mathbf{k}\uparrow}\gamma_{\mathbf{k}\uparrow} - \gamma^{\dagger}_{-\mathbf{k}\downarrow}\gamma_{-\mathbf{k}\downarrow}\right) \tag{2.2}$$

where the γ-operators are quasiparticle operators given by $\left(\begin{smallmatrix}\gamma_{\mathbf{k}\uparrow}\\ \gamma^{\dagger}_{-\mathbf{k}\downarrow}\end{smallmatrix}\right) = \left(\begin{smallmatrix}u & v\\ -v & u\end{smallmatrix}\right)\left(\begin{smallmatrix}c_{\mathbf{k}\uparrow}\\ c^{\dagger}_{-\mathbf{k}\downarrow}\end{smallmatrix}\right)$. u and v are the superconducting coherence factors describing the electron and hole part of the quasiparticle states respectively. The excitation energies are given by $E_{\mathbf{k}} = \sqrt{\varepsilon^2_{\mathbf{k}} + |\Delta_{\mathbf{k}}|^2}$, and the density of states of simple s-wave superconductors is

$$\frac{N_s(E)}{N(0)} = \frac{d\varepsilon}{dE} = \begin{cases} \frac{E}{(E^2-\Delta^2)^{\frac{1}{2}}} & E > \Delta \\ 0 & E < \Delta \end{cases} \tag{2.3}$$

The quantity Δ is called the superconducting gap parameter, and is given by

$$\Delta_{\mathbf{k}} = -\sum_{\mathbf{k}'} V_{\mathbf{k}\mathbf{k}'} \Delta_{\mathbf{k}'} \frac{\tanh\left(\frac{\beta E_{\mathbf{k}'}}{2}\right)}{2E_{\mathbf{k}'}} \tag{2.4}$$

This is the BCS gap-equation. The physical interpretation of Δ is a gap in the quasiparticle spectrum at the Fermi surface. There are available two-particle states for Cooper pairs at the Fermi level, while the quasiparticles must have an energy greater than the superconducting gap.

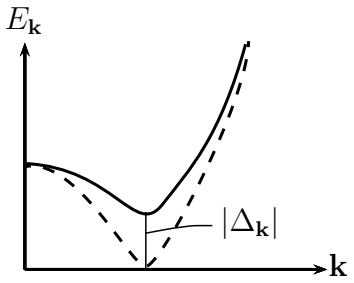

Figure 2.2: A sketch of the excitation spectrum of the superconducting state (solid line) compared to the excitation spectrum of the normal state (dashed line). The energies are measured relative to the chemical potential μ.

As we see at the end of section 3.2 the quasiparticle states of the superconductor will be a mix between electron states and hole states. The wave functions in the superconductor will then consist of an electron-like part and a hole-like part, which distinguishes the superconductor from a semiconductor.

2.2 Superconducting hybrid structures

In our context hybrid structures are systems built up by both superconductors and other materials. There have been many papers of hybrid structures built up by normal metals and superconductors, one of the most famous being Blonder, Tinkham and Klapwijk's paper from 1982 [6]. We are going to examine structures which contain both superconducting and magnetic elements. This alters some of the transport mechanisms, but the principles are the same and will be explained in this section. All the considered mechanisms take place for energies below the superconducting gap energy. Above this energy an incoming particle may be transmitted via the quasiparticle states in the superconductor. Normal reflection is present for all energies.

2.2.1 Andreev reflection

The first and simplest process is Andreev reflection [7]. Across an N-S junction energy must be conserved. Since no one-particle states with energies lower than the energy gap exist in superconducting materials, incoming particles with these energies can not be transmitted into the quasiparticle states of the superconductor. However, there is still a possibility for transmission of charge. As already explained the current in superconductors is carried by Cooper pairs at the Fermi energy. An incoming electron with momentum q^+, spin σ and energy $E_F + \varepsilon_{\mathbf{q}}$ will pair up with an electron with momentum $-q^-$, spin $-\sigma$ and energy $E_F - \varepsilon_{\mathbf{q}}$. Together their total energy equals $2E_F$, and the pair will tunnel into the superconducting layer as a Cooper pair with momenta $\mathbf{k}$ and $-\mathbf{k}$ and spin σ and $-\sigma$. An empty state is left at $-q^-$ in the metal. This corresponds to a hole at q^- with spin $-\sigma$. This hole will be retroreflected in the metal. A hole in the spin down band is the same as a missing electron in the spin down band, which effectively is the same as a spin up excitation. The hole in the $-\sigma$ band will then have spin σ.

2.2.2 Non-local transport mechanisms

When the superconductor is placed between two metals there are also some non-local processes taking place [8]. For a given energy the possible wave numbers in a superconductor are $k_\pm = \sqrt{2m(\mu \pm \sqrt{\Delta^2 - E^2})}$. At an excitation energy less than the superconducting gap there is an imaginary part in the momentum. An electron arriving at the junction with too low energy will then result in an evanescent

wave in the superconductor. The wave decays over a length of same order as the superconducting coherence length.

If the superconducting film has a width that is less than the coherence length the evanescent wave will have a finite amplitude when arriving at the second interface. Here it will occupy a single particle state if such a state is available. This process is called elastic cotunneling and is coherent tunneling from one metal through virtual quasiparticle states in the superconductor into the other metal.

The last process is called crossed Andreev reflection and are similar to normal Andreev reflection. When the width of the superconducting film is less than the coherence length the evanescent wave of an incoming electron will overlap with the evanescent wave of an electron in the other metal. These two electrons may then form a Cooper pair and following the discussion of normal Andreev reflection a hole will be backreflected in the second metal.

Chapter 3

Superconducting and magnetic correlations

In both the systems we are going to consider the interplay between superconducting and magnetic correlations are important. By including magnetic fields and potentials the two spin bands will no longer be degenerate, and the spin dependence of the processes described in the previous chapter become more apparent. Before we can start to consider the actual systems we are going to investigate, a theoretical foundation is necessary. In this chapter we will look at the most important theory for superconducting and magnetic correlations.

3.1 Superconductor in a magnetic field

One of the two defining properties of a superconductor is the Meissner effect. It is the complete expulsion of an applied magnetic field from the bulk of the superconductor. Superconductivity and magnetism are thus two competitive properties. When the strength of the applied magnetic field is increased beyond a critical field strength H_C the Meissner effect breaks down. The superconductor shows two distinct behaviours as the field is increased beyond this critical field strength. The simplest behaviour is shown by the type I superconductors, which return to the normal state of full penetration of magnetic field. Type II superconductors on the other hand have two critical field strengths. At H_{C1} the state goes from the superconducting state to a state of partial penetration of magnetic flux. The penetration increases continously until full penetration (normal state) at H_{C2}.

Even though the magnetic field is expelled from the bulk of the superconductor at field strengths lower than the critical field, the magnetic field is not completely excluded at the surface. Within a distance, λ, called the London penetration depth, a small magnetic field can be measured.

3.1.1 Singlet and triplet superconductivity

The normal BCS-type superconductor is a so called spin-singlet superconductor. They are characterized by having Cooper pairs with zero center of mass momentum, zero total spin (a spin-singlet) and a charge of $2e$ as current carriers. An applied magnetic field can destroy singlet superconductivity by the means of the orbital effect and the paramagnetic effect. The orbital effect makes use of the Lorentz force. Since the two electrons in the Cooper pair have opposite momenta the Lorentz force will act in different directions pulling the pair apart. The paramagnetic effect causes the spins to align along the direction of the applied field.

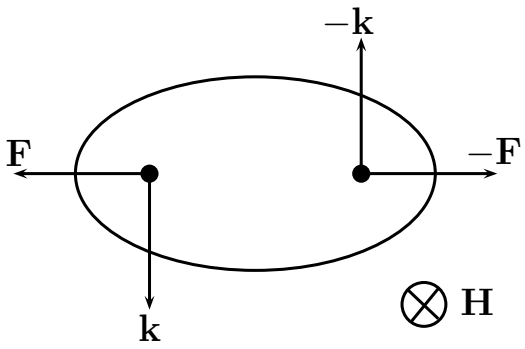

Figure 3.1: The applied magnetic field pulls the pair apart because the two electrons have opposite momentum. This is the orbital effect.

Another form of superconductivity is found in the triplet superconductors. They are characterized by that the electron pair inhabits a spin-triplet state, that is a state with a total spin of 1. Such superconductors may require another form of attractive interaction than the phonon mediated interaction in singlet superconductors. Two of the three spin-triplet states have parallel spins. These states will not be destroyed by the paramagnetic effect since the spins already are aligned. In such superconductors one may find that both superconducting and ferromagnetic properties are present at the same time [9].

When the paramagnetic effect is too large for spin-singlet superconductivity to survive the Cooper pair has two options not too be destroyed. It must either turn into an equal-spin pair or it can keep the spins antiparallel ant get a non-zero center of mass momentum. The exchange splitting of the spin bands leads to a shift in the momenta at the Fermi surface that differs for the spin up and the spin down band; $\mathbf{k_{F\uparrow}} = \mathbf{k_F} + \frac{\mathbf{Q}}{2}$ and $\mathbf{k_{F\downarrow}} = \mathbf{k_F} - \frac{\mathbf{Q}}{2}$. The center of mass momentum will then be $\pm\mathbf{Q}$. This leads to a modulation of the pair amplitude with position $\mathbf{R}$, and the result is a state that is a mixture between spin-singlet states ($\uparrow\downarrow - \downarrow\uparrow$) and spin-triplet states with antiparallel spins ($\uparrow\downarrow + \downarrow\uparrow$). This state is called an FFLO-state [10, 11]. It is theoretically shown that this state could exist in ferromagnetic superconductors.

3.1.2 Clogston-Chandrasekhar limit

As already mentioned there are two magnetic effects destroying the superconducting state, orbital and paramagnetic (the Zeeman effect). Usually it is the orbital effect that dominates over the paramagnetic one and thus is the most restrictive. The orbital effect can be directly related to the vortex formation in type II superconductors. At field strengths larger than H_{C1} the magnetic field penetrates the superconductor in form of magnetic vortices, so called Abrikosov vortices, of quantized circulation [12]. Superconductivity is destroyed at the center of each vortex, where the density of Cooper pairs is zero. The supercurrent is travelling around the vortex cores. Hence the magnetic field goes to zero when moving away from the center of each vortex. As a result of these vortices some Cooper pairs will break and energy is lost destabilizing the superconducting state. Increasing the field beyond H_{C2} there will be a transition to a normal state. In type I superconductors the transition goes directly from the state of no penetration to the normal state.

For some geometries it is possible to suppress the orbital effect. This is achieved by applying an external magnetic field in-plane of a thin superconducting film [13, 14]. The radius of the vortex is of the same order as the penetration depth while the radius of the vortex core is described by the superconducting coherence length. To suppress the orbital effect the thickness of the film must be much smaller than the size of the vortex core. In a type II superconductor $\xi < \lambda$, where ξ is the coherence length and λ is the penetration depth. By choosing a geometry where the superconductor is thinner than the coherence length there will be no room to form vortices and superconductivity can coexist with the magnetic field up to a critical exchange field h known as the Clogston-Chandrasekhar limit [15, 16].

The limiting value can be found by setting the polarization energy of the normal electron gas $\frac{\chi_n H^2}{2}$ equal to the condensation energy of the superconductor $\frac{N(0)\Delta_0^2}{2}$, where χ_n is the spin susceptibility, $N(0)$ is the normal density of states and Δ_0 is the zero temperature gap. Using $\chi_n = g_s \mu_B^2 N(0)$, where $g_s \approx 2$ is the gyromagnetic factor and μ_B is the Bohr magneton, the limiting value is obtained $H = \frac{\Delta_0}{\sqrt{2}\mu_B}$ or in terms of the field energy

$$h = \frac{\Delta_0}{\sqrt{2}} \tag{3.1}$$

This critical field strength is valid for s-wave superconductors of both type I and II. Type I superconductors do not let magnetic flux penetrate further then the penetration depth, and we must then have a superconducting film with thickness much less than the penetration depth. As $\lambda < \xi$ for type I superconductors, a general requirement for coexistence between superconductivity and the magnetic field is that the thickness of the film is much less than the coherence length. Normal s-wave superconductors will not be polarized when the field strength is lower than the Clogston-Chandrasekhar limit. A thin sample will however allow the field to penetrate the sample homogenously and induce a Zeeman splitting of the quasiparticle bands.

3.1.3 Zeeman effect

A single particle with charge q and mass m in a homogenous magnetic field B along the z-direction is subject to the following magnetic perturbation

$$H' = -\frac{q}{2m}BL_z + \frac{q^2B^2}{8m}(x^2+y^2) - \frac{g_s q}{2m}BS_z \tag{3.2}$$

The second term can be small compared to the other two if the magnetic field is not to strong, and can be neglected. When we are looking at a thin superconducting film with an in-plane magnetic field we have concluded that the orbital effect is negligible compared to the paramagnetic effect caused by the spin. We can then remove the first term and are left with the last one. This is a Zeeman interaction that can spin polarize the system and split the energy levels for excitations with spin parallel and antiparallel to the magnetization vector. The energy splitting is given by twice the Zeeman energy.

The magnetic moment of a particle is a quantity that determines the torque a magnetic field will exert on the particle. Electrons have an intrinsic magnetic moment commonly known as the electron spin **S**. Placed in a magnetic field the spin of the electron will try to align with the field lines giving a paramagnetic effect. An electron circulating an atom has also a magnetic moment, μ_L associated with the orbital angular momentum. It may be incorparated in the model by using an effective magnetic moment μ_{eff} taking account of both the spin and the orbital angular momentum. In principle this will only change the required field strength necessary for giving a particular field energy.

For an electron with mass m and charge $-e$ placed in a homogenous magnetic field along the z-direction the energy associated with the magnetic moment will be $-\mu_{\mathbf{S}} \cdot \mathbf{H}$, where the spin magnetic moment is given by

$$\mu_{\mathbf{S}} = -g_S \frac{e}{2m}\mathbf{S} \tag{3.3}$$

The additional energy to the electron will then be

$$\Delta E = -\mu_{\mathbf{S}} \cdot \mathbf{H} = \frac{1}{2}\frac{g_S e}{2m}HS_z = g_S\mu_B H\sigma_Z \tag{3.4}$$

where $\mu_B = \frac{e\hbar}{2m} = 0.579 \cdot 10^{-4}$ eV/T is the Bohr magneton and $\sigma_z = \pm 1$ (from here on we will drop the z-index). Introducing the Zeeman energy $h = \frac{1}{2}g_S\mu_B H$ we can write in second qantized form

$$H_{Zeeman} = -\sum_{\mathbf{k},\sigma} h\sigma c^\dagger_{\mathbf{k}\sigma}c_{\mathbf{k}\sigma} \tag{3.5}$$

This term will come as an additional term in the BCS-Hamiltonian, (2.1).

3.2 Zeeman split superconductor

We are now interested in finding the wave functions and energy excitations of a Zeeman split superconductor. The treatment of such superconductors follows the same procedure as the original BCS theory. The difference is the introduction of the Zeeman field which give an additional term (3.5) to the BCS-Hamiltonian.

The Hamiltonian with Zeeman field is given by:

$$H = \sum_{\mathbf{k},\sigma} \varepsilon_{\mathbf{k}\sigma} c^\dagger_{\mathbf{k}\sigma} c_{\mathbf{k}\sigma} + \sum_{\mathbf{k},\mathbf{k}',\sigma,\sigma'} V_{\mathbf{k}\mathbf{k}'} c^\dagger_{\mathbf{k}\sigma} c^\dagger_{-\mathbf{k}\sigma'} c_{-\mathbf{k}'\sigma'} c_{\mathbf{k}'\sigma} \tag{3.6}$$

where the usual kinetic energy term is exchanged for a spin dependent term given by $\varepsilon_{\mathbf{k}\sigma} = \varepsilon_{\mathbf{k}} - \sigma h$. Here h is the Zeeman energy expressed by $h = \frac{1}{2} g_s \mu_B B$. The rest of the terms are defined as in equation (2.1).

At this point we will do a mean-field approximation to simplify the potential term. With a mean-field approximation we can write the product of four creation and annihilation operators as a sum of terms with a product of two operators. The approximation is justified by the fact that the effective interaction potential $V_{\mathbf{k}\mathbf{k}'}$ we are considering is an interaction between particles close in space, which means a long-range $\mathbf{k}$-space potential. We write

$$c_{-\mathbf{k}\sigma'} c_{\mathbf{k}\sigma} = b_{\mathbf{k}\sigma\sigma'} + \underbrace{c_{-\mathbf{k}\sigma'} c_{\mathbf{k}\sigma} - b_{\mathbf{k}\sigma\sigma'}}_{\delta_{bk\sigma\sigma'}} \tag{3.7}$$

Here the statistical meanvalue $b_{\mathbf{k}\sigma\sigma'} = \langle c_{-\mathbf{k}\sigma'} c_{\mathbf{k}\sigma} \rangle$ is introduced. This is inserted into the second term in (3.6). If we neglect all terms of second order and higher in $\delta_{bk\sigma\sigma'}$ we get

$$H = \sum_{\mathbf{k}\sigma} (\varepsilon_{\mathbf{k}} - \sigma h) c^\dagger_{\mathbf{k}\sigma} c_{\mathbf{k}\sigma} + \sum_{\mathbf{k},\mathbf{k}',\sigma,\sigma'} V_{\mathbf{k}\mathbf{k}'} \left[b^\dagger_{\mathbf{k}\sigma\sigma'} c_{-\mathbf{k}'\sigma'} c_{\mathbf{k}'\sigma} + b_{\mathbf{k}'\sigma\sigma'} c^\dagger_{\mathbf{k}\sigma} c^\dagger_{-\mathbf{k}\sigma'} - b^\dagger_{\mathbf{k}\sigma\sigma'} b_{\mathbf{k}'\sigma\sigma'} \right] \tag{3.8}$$

We now introduce the superconducting gap parameter by the relations

$$\begin{aligned} \Delta^\dagger_{\mathbf{k}'\sigma\sigma'} &= -\sum_{\mathbf{k}} V_{\mathbf{k}\mathbf{k}'} b^\dagger_{\mathbf{k}\sigma\sigma'} \\ \Delta_{\mathbf{k}\sigma\sigma'} &= -\sum_{\mathbf{k}'} V_{\mathbf{k}\mathbf{k}'} b_{\mathbf{k}'\sigma\sigma'} \end{aligned} \tag{3.9}$$

The mean-field approximation of the Hamiltonian for a Zeeman split superconductor can then be written

$$H = \sum_{\mathbf{k}\sigma} (\varepsilon_{\mathbf{k}} - \sigma h) c^\dagger_{\mathbf{k}\sigma} c_{\mathbf{k}\sigma} - \sum_{\mathbf{k}\sigma\sigma'} \left(\Delta^\dagger_{\mathbf{k}\sigma\sigma'} c_{-\mathbf{k}\sigma'} c_{\mathbf{k}\sigma} + \Delta_{\mathbf{k}\sigma\sigma'} c^\dagger_{\mathbf{k}\sigma} c^\dagger_{-\mathbf{k}\sigma'} - \Delta_{\mathbf{k}\sigma\sigma'} b^\dagger_{\mathbf{k}\sigma\sigma'} \right) \tag{3.10}$$

A chemical potential can be introduced into the Hamiltonian by $\varepsilon_{\mathbf{k}} \to \varepsilon_{\mathbf{k}} - \mu$. The many-particle problem is now reduced to a self-consistent one-particle problem that can be solved exactly and non-perturbatively.

The next step will be to write the Hamiltonian in matrix form.

$$H = H_0 + \sum_{\mathbf{k}} \phi^\dagger_{\mathbf{k}} \underbrace{\begin{pmatrix} \varepsilon_{\mathbf{k}} - h & 0 & 0 & \Delta_{\mathbf{k}} \\ 0 & \varepsilon_{\mathbf{k}} + h & -\Delta_{\mathbf{k}} & 0 \\ 0 & -\Delta^\dagger_{\mathbf{k}} & -\varepsilon_{\mathbf{k}} + h & 0 \\ \Delta^\dagger_{\mathbf{k}} & 0 & 0 & -\varepsilon_{\mathbf{k}} - h \end{pmatrix}}_{A_{\mathbf{k}}} \phi_{\mathbf{k}} \tag{3.11}$$

As $\Delta_{\mathbf{k}\sigma-\sigma}$ and $b^\dagger_{\mathbf{k}\sigma-\sigma}$ are not operators $H_0 = \sum_{\mathbf{k}} \left(\varepsilon_{\mathbf{k}} + h + \Delta_{\mathbf{k}\uparrow\downarrow} b^\dagger_{\mathbf{k}\uparrow\downarrow} + \Delta_{\mathbf{k}\downarrow\uparrow} b^\dagger_{\mathbf{k}\downarrow\uparrow} \right)$ is just a constant energy term. In writing down (3.11) we have chosen the basis $\phi_{\mathbf{k}} = \left(c_{\mathbf{k}\uparrow} \; c_{\mathbf{k}\downarrow} \; c^\dagger_{-\mathbf{k}\uparrow} \; c^\dagger_{-\mathbf{k}\downarrow} \right)^{\mathrm{T}}$.

We find the eigenvalues by solving the characteristic equation $|A - \lambda \mathbb{I}| = 0$. Doing this we end up with four eigenvalues given by $\lambda = \pm E_{\mathbf{k}\sigma} = \pm \left(\sqrt{\varepsilon^2_{\mathbf{k}} + \Delta^2} - \sigma h \right)$.

As with the normal BCS superconductor treatment we end up with an energy gap. The difference is that in addition there is a splitting between bands corresponding to spin up particles and spin down particles. For each spin species there is a gap of 2Δ between the positive and negative energies, and between the positive energies of spin up and spin down particles there is a splitting of $2h$. A sketch of the positive excitation energies are given in Fig. 3.2.

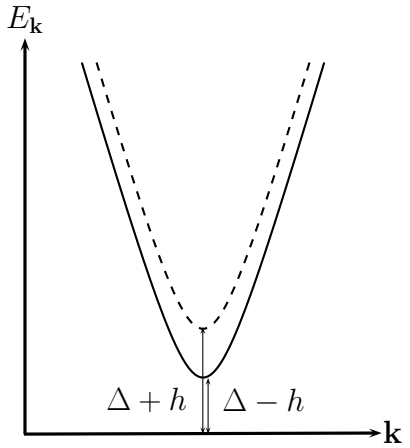

Figure 3.2: The positive excitation spectrum of the spin up particles (solid line) and spin down particles (dashed line) relative to the chemical potential μ. The splitting between the bands is $2h$ where h is the exchange field energy.

To find the wave functions corresponding to particles with different spins it is necessary to diagonalize (3.11). This task can be simplified by observing that the four-component system can be decoupled into two two-component systems. We use a basis $\phi_{\mathbf{k}\sigma} = \left(c_{\mathbf{k}\sigma} \; c^\dagger_{-\mathbf{k}-\sigma} \right)^{\mathrm{T}}$ where $\sigma = \pm 1$ represents spin up and down respectively. The new $2x2$-matrix which holds for both two-component systems then reads

$$A_{\mathbf{k}\sigma} = \begin{pmatrix} \varepsilon_{\mathbf{k}} - \sigma h & \sigma\Delta \\ \sigma\Delta^{\dagger} & -\varepsilon_{\mathbf{k}} - \sigma h \end{pmatrix} \tag{3.12}$$

To diagonalize $A_{\mathbf{k}\sigma}$ we introduce new fermion operators by the transformation $\tilde{\phi_{\mathbf{k}}} = \begin{pmatrix} \gamma_{\mathbf{k}\sigma} \\ \gamma^{\dagger}_{-\mathbf{k}-\sigma} \end{pmatrix} = \begin{pmatrix} u_{\sigma} & v_{-\sigma} \\ -v_{-\sigma} & u_{\sigma} \end{pmatrix} \begin{pmatrix} c_{\mathbf{k}\sigma} \\ c^{\dagger}_{-\mathbf{k}-\sigma} \end{pmatrix}$, where $u_{\sigma}^2 + v_{-\sigma}^2 = 1$. This represents a rotation of the original basis. u and v are called the superconducting coherence factors and are defined by

$$\begin{aligned} u_{\sigma}^2 &= \frac{1}{2}\left(1 + \frac{\sqrt{(E+\sigma h)^2 - \Delta^2}}{E + \sigma h}\right) \\ v_{-\sigma}^2 &= \frac{1}{2}\left(1 - \frac{\sqrt{(E+\sigma h)^2 - \Delta^2}}{E + \sigma h}\right) \end{aligned} \tag{3.13}$$

The total Hamiltonian of the system can then be written

$$H = H_0 + \sum_{\mathbf{k}\sigma} \tilde{\phi^{\dagger}_{\mathbf{k}\sigma}} \begin{pmatrix} \sqrt{\varepsilon_{\mathbf{k}}^2 + \Delta^2} - \sigma h & 0 \\ 0 & -\sqrt{\varepsilon_{\mathbf{k}}^2 + \Delta^2} - \sigma h \end{pmatrix} \tilde{\phi_{\mathbf{k}\sigma}} \tag{3.14}$$

The coherence factors give information about the quasiparticle states of the superconductor. Since we could decouple the Hamiltonian there will be no correlation between spin σ electrons and spin σ holes. Instead of the four-component wave vector that one usually needs when working with spin dependent particles we can therefore use a two component wave vector composed of a spin σ electron part and a spin $-\sigma$ hole part. The wave function is then given as a sum of a electron-like part and a hole-like part

$$\psi = \psi_e \begin{pmatrix} u_{\sigma} \\ v_{-\sigma} \end{pmatrix} e^{i\mathbf{k}_{\sigma}\mathbf{x}} + \psi_h \begin{pmatrix} v_{-\sigma} \\ u_{\sigma} \end{pmatrix} e^{-i\mathbf{k}_{\sigma}\mathbf{x}} \tag{3.15}$$

3.3 Proximity effect

When a superconductor is brought in contact with a material that is not a superconductor some physical properties may change in the materials. In the area around the junction the wave function of the superconductor side influences the wave function of the other material and vice versa. This is called the proximity effect. The reason that the wave functions influence eachother is tunneling. Cooper pairs may tunnel into the other material while electronic excitations tunnel the other way. Superconductivity will then be suppressed over a distance of the order of the coherence length from the junction. The effect will be reduced by an insulating barrier between the two sides.

If the other material is a ferromagnet the proximity effect will lead to correlations between superconductivity and magnetism. The pair amplitude of the superconductor will leak into the ferromagnet. The spin splitting of the electron states in the ferromagnet will give Cooper pairs with a finite center of mass momentum as in the

FFLO state. The FFLO amplitudes oscillate and penetrate over a length scale that decreases fast with increasing exchange field in the ferromagnet [17]. Because the proximity effect takes place on both sides of the interface there will also be a mixing of triplet and singlet Cooper pairs on the superconductor side of the junction.

To be able to make strongly spin-polarized currents the exchange field of the ferromagnet must be strong. This will give a short-ranged proximity effect. What we want is a long-ranged proximity effect coexisting with the spin properties. Such long-ranged proximity amplitudes could lead to long-ranged spin-polarized supercurrents. The two electrons of the Cooper pair would then need to have equal spin. A possible solution will be spin-active interfaces.

The scattering potential at the interface between a ferromagnet and a superconductor can in general be spin-dependent. This can be a result of the energy splitting of the spin bands in the ferromagnetic region [18]. Transmission probabilities for spin up and spin down electrons will then differ both in magnitude and phase, and one of the spin species will be favoured tunneling-wise. The phase shifts may introduce spin-triplet correlations. If the spin-active potential has a component in a direction that is not parallel or antiparallel to the polarization of the magnetic field of the ferromagnet there will be spin-flip processes at the interface. There will be a certain probability that incoming spin up particle will be reflected or transmitted as a particle with spin down. A spin-active potential may be modelled by a function of the following form

$$\mathbf{V} = \boldsymbol{\sigma}\mathbf{h} \tag{3.16}$$

where $\boldsymbol{\sigma}$ is the vector of Pauli matrices and $\mathbf{h}$ is the magnetization vector. In chapter 5 we will use the concept of spin-active interfaces when examining the magnetoresistance in F-S-F hybrid structure.

Chapter 4

Zeeman split superconductors and spin polarization

A system built up by a thin superconducting film placed between two semi-infinite normal metals is a system that has been given a lot of attention in the literature, eg. [19]. In this first of two main chapters we will look at a variant of this system. We apply a static and uniform magnetic field, H, to the superconducting part of the junction. The thickness of the superconducting film is chosen to be less than the superconducting penetration depth. From the arguments of chapter 3 we then know that the field will penetrate the bulk of the superconductor homogenously, and superconductivity will coexist with the Zeeman field up to the Clogston-Chandrasekhar limit (3.1). This will result in a Zeeman splitting of the two spin bands as has been previously showed. Hopefully this splitting will give rise to new features compared to the same system with a normal superconductor. Of special interest is the spin properties of the structure. A sketch of the setup is given in Fig. 4.1.

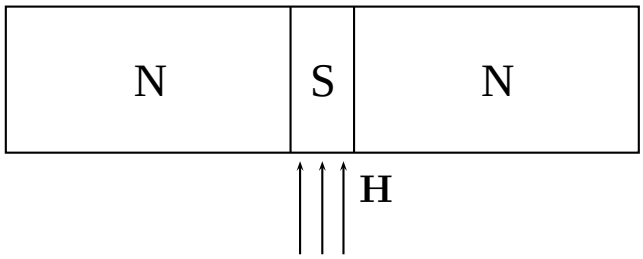

Figure 4.1: A superconducting film of width much less than the penetration depth is placed between to semi-infinite normal metals. An in-plane magnetic field with field strength lower than the Clogston-Chandrasekhar limit is applied. This gives a Zeeman splitting of the excitation spectrum of the superconductor.

To ensure ballistic transport the transverse dimension of the junction is chosen to be much smaller than the mean free path in the normal metal and the coherence length of the superconductor. This type of junction is called a Sharvin contact [20]. We can then consider acceleration of particles without needing to consider other

scattering events than those at the juction. Scattering potentials other than at the N-ZS interfaces will be neglected.

Since the superconducting material is just a thin film placed between two semi-infinite normal metals, it is the metals that will behave as reservoirs. There will therefore be an inverse proximity effect taking place which suppresses superconductivity close to the metals giving a varying order parameter. To simplify the calculations we will not consider this effect.

For simplicity we will also only consider one-dimensional problems and s-wave superconductors of type I. Examples of such superconductors are aluminium (Al) and lead (Pb). Pure aluminium has a coherence length of 1600 nm and a penetration depth of 16 nm [21]. To get a Zeeman splitted superconductor the width of the superconducting film should then be much less than 16 nm, giving a ratio between the coherence length and the width of the superconductor to be of the order of 10^{-2}. Pure lead on the other hand has $\lambda = 37$ nm and $\xi = 83$ nm [21]. Then one need $\frac{L}{\xi} \sim 10^{-1}$. As we will see this ratio affects the different transport coefficients of the system and will hence have some impact upon the properties of the junction.

4.1 Bogoliubov deGennes equations

At the interface between the metal and the superconductor there will be some kind of insulating barrier, which may be a result of an oxide layer at the surfaces. This introduces a potential barrier at the junction. Techniques exist to make the junction more or less transparent. With a highly transparent junction particles can propagate freely through the junction. The less transparent the junction is the higher will the potential barrier be. From quantum mechanics we know that particles then will have to tunnel between the two sides. These differences must be taken into account when calculating the transport properties of our system. The usual method is the one explained in the classical paper on the 'normal metal - superconductor' system by Blonder, Tinkham and Klapwijk (BTK) [6]. They introduced a delta-barrier with a given strength. By changing the strength of the barrier one can distinguish between junctions with high and low transparency, as well as the intermediate regime. Setting the barrier strength to zero gives a perfect junction.

To set up the wave functions in the different parts of the system we need to look at the excitation energies for particles travelling in them. The two metals are assumed to be of the same type. The exchange field energy is less than $\frac{\Delta_0}{\sqrt{2}}$. Since $\Delta_0 \sim 1$ meV for a typical type I s-wave superconductor the field is far to weak to split the energy bands of the metals. The wave functions in the metals will then be well approximated by ususal free electron wave functions.

In the superconductor the contribution of h can give imaginary parts in the wave number, and h can not be neglected. The wave function in the superconducting film will be a solution of the Bogoliubov deGennes equations. These equations may be found from (3.11) following the same procedure as [22]. As for the Hamiltonian we can decouple the equations into a pair containing electron-like particles in the

spin σ band and hole-like particles in the spin $-\sigma$ band. If $\psi_\sigma(x,t)$ represents the electron-like part and $\psi^\dagger_{-\sigma}(x,t)$ represents the hole-like part the Bogoliubov deGennes equations reads

$$\begin{pmatrix} H_0 - \sigma h & \Delta \\ \Delta^\dagger & -H_0 - \sigma h \end{pmatrix} \begin{pmatrix} \psi_\sigma(x,t) \\ \psi^\dagger_{-\sigma}(x,t) \end{pmatrix} = i\frac{\partial}{\partial t} \begin{pmatrix} \psi_\sigma(x,t) \\ \psi^\dagger_{-\sigma}(x,t) \end{pmatrix} \tag{4.1}$$

where $H_0 = -\frac{\nabla^2}{2m} - \mu(x) - V(x)$. $\mu(x)$ is the chemical potential, while $V(x)$ is the barrier potential. We see that the Bogoliubov deGennes equations reduce to two decoupled Schrödinger equations when $\Delta \to 0$. As trial solutions we choose plane waves with energy $E_{\mathbf{k}\sigma}$; $\psi_\sigma(x,t) = u_\sigma e^{i\mathbf{kx} - iE_{\mathbf{k}\sigma}t}$ and $\psi^\dagger_{-\sigma}(x,t) = v_{-\sigma} e^{i\mathbf{kx} - iE_{\mathbf{k}\sigma}t}$. Solving the coupled system of equations give the excitation energy of the BCS quasiparticles

$$E_{\mathbf{k}\sigma} = \pm\left(\sqrt{\left(\frac{k^2_{\sigma\pm}}{2m} - \mu\right)^2 + \Delta^2} - \sigma h\right) \tag{4.2}$$

There are four wave numbers, $\pm\mathbf{k}_{\sigma\pm}$, that give the same excitation energy. These are

$$\pm k_{\sigma\pm} = \pm\sqrt{2m\left(\mu \pm \sqrt{(E+\sigma h)^2 - \Delta^2}\right)} \tag{4.3}$$

The first sign-choice gives the propagation direction of the wave while the second determines if it is an electron-like or hole-like wave. σ is the spin of the incoming particle.

The prefactors u_σ and $v_{-\sigma}$ can be defined in the same way as the BCS coherence factors of equation (3.13). Wave numbers larger than the Fermi momentum, $|\mathbf{k}_+| > |\mathbf{k_F}|$, will make $u_\sigma > v_{-\sigma}$ and give electron-like quasiparticles, while wave numbers smaller than the Fermi momentum, $|\mathbf{k}_-| < |\mathbf{k_F}|$, make $u_\sigma < v_{-\sigma}$ and give hole-like quasiparticles.

4.2 Transport coefficients

When we send an electron into the junction we can observe the same processes as in the N-S-N junction: Andreev reflection, normal reflection, transmission as an electron and transmission as a hole. Let the probability amplitudes for these processes be, a, b, c and d respectively. The probability amplitudes for the intermediate quasiparticle states in the superconductor are given by e, f, g and h. In Fig. 4.2 a schematic energy diagram for the junction is given. As a barrier potential we choose a delta potential at each interface; $V(x) = W(\delta(x) + \delta(x-L))$ where W is the strength of the potential and L is the thickness of the superconducting film. Based on the arguments in the previous section the wave functions in the three parts will be

$$\begin{aligned}
\psi_{N1} &= \begin{pmatrix}1\\0\end{pmatrix} e^{iq_+x} + a\begin{pmatrix}0\\1\end{pmatrix} e^{iq_-x} + b\begin{pmatrix}1\\0\end{pmatrix} e^{-iq_+x}, x < 0 \\
\psi_{ZS} &= \left(ee^{ik_{\sigma+}x} + fe^{-ik_{\sigma+}x}\right)\begin{pmatrix}u_\sigma\\v_{-\sigma}\end{pmatrix} + \left(ge^{ik_{\sigma-}x} + he^{-ik_{\sigma-}-x}\right)\begin{pmatrix}v_{-\sigma}\\u_\sigma\end{pmatrix}, 0 < x < L \\
\psi_{N2} &= c\begin{pmatrix}1\\0\end{pmatrix} e^{iq_+x} + d\begin{pmatrix}0\\1\end{pmatrix} e^{-iq_-x}, x > L
\end{aligned}$$

with $k_{\sigma\pm}$ given by (4.3) and $q_\pm = q_F\sqrt{1 \pm \frac{E}{E_F}}$.

The boundary conditions are given by $\psi(0^+) = \psi(0^-)$, $\psi(L^+) = \psi(L^-)$, $\psi'(0^+) - \psi'(0^-) = 2mW\psi(0)$ and $\psi'(L^+) - \psi'(L^-) = 2mW\psi(L)$ [23, ch. 3]. This gives a system of 8 equations with 8 unknowns.

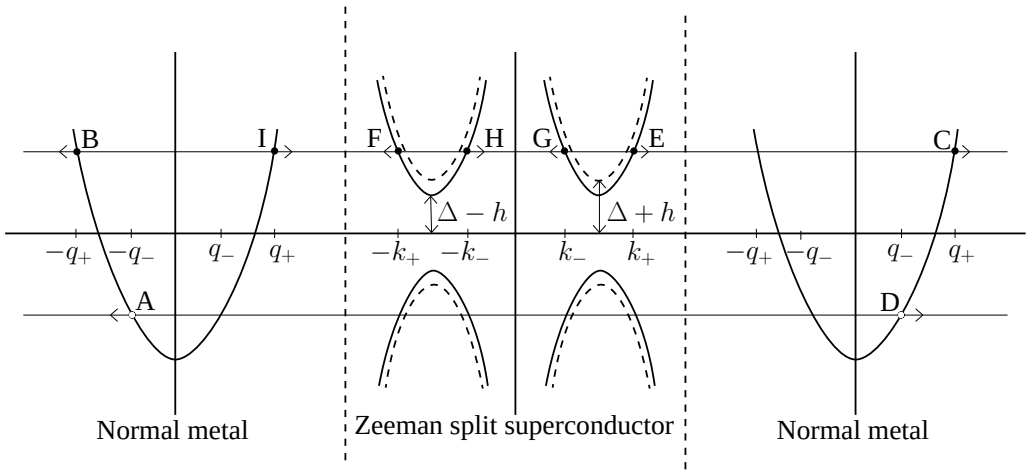

Figure 4.2: Schematic energy diagram for the N-ZS-N junction. I represents an incoming electron, A is an Andreev reflected hole, B is a reflected electron, C is a transmitted electron and D is a transmitted hole. E, F, G and H represents quasiparticles in the superconductor. The holes are here illustrated by the missing electrons and thus have opposite momenta of what is indicated by the figure.

It is difficult to solve the system analytically without some approximations. A natural assumption is that $\frac{E}{E_F} \ll 1$ and $\frac{\Delta}{E_F} \ll 1$. We can then introduce the approximations $k^+ \approx k^- \approx k_F$ and $q^+ \approx q^- \approx q_F$. These approximations are justified since the interesting energies are of the same order of magnitude as the superconducting gap. The gap is known to be small compared with the Fermi energy ($\frac{\Delta}{E_F} \sim 10^{-3}$) and the momenta will then be close to the Fermi momentum. These approximations are performed everywhere except in the exponents where the neglection of small terms may lead to the loss of oscillations in the transport coefficients. The probability amplitudes that are of interest is a, b, c and d.

To simplify the notation it is convenient to introduce the following quantities $\zeta_- = (k_+ - k_-)L$, $\zeta_+ = (k_+ + k_-)L$, $\kappa = \frac{q_F}{k_F}$, $A_\pm = K_1 \pm K_2$, $B_\pm = 1 \pm K_1K_2$, $C_+ = 2K_2$, $D_\pm = 1 \pm K_2^2$, $K_1 = \kappa + iZ$, $K_2 = \kappa - iZ$, $Z = \frac{2mW}{k_F}$ and $\Omega = \sqrt{(E + \sigma h)^2 - \Delta^2}$. The common denominator of all the probability amplitudes is given by

$$\begin{aligned}\Gamma = \Delta^2 A_+^2 \quad &- \quad ((E+\sigma h)^2 A_+^2 + \Omega^2 B_+^2)\cos\zeta_- + \Omega^2(A_-^2 + B_-^2)\cos\zeta_+ \\ &+ \quad 2i\Omega E A_+ B_+ \sin\zeta_- - 2i\Omega^2 A_- B_- \sin\zeta_+ \end{aligned} \tag{4.4}$$

After solving the system the expressions for the probability amplitudes can be written

$$\begin{aligned}
a &= \frac{4\kappa\Delta \sin\left(\frac{\zeta_-}{2}\right)}{\Gamma}\left[(E+\sigma h)A_+ \sin\left(\frac{\zeta_-}{2}\right) + iB_+\Omega\cos\left(\frac{\zeta_-}{2}\right)\right] \\
b &= \frac{1}{\Gamma}\left[\Omega^2 B_+ D_- \cos\zeta_- + \Omega^2(A_- C_+ - B_- D_+)\cos\zeta_+\right. \\
&\quad \left. - i\Omega(E+\sigma h)A_+ D_- \sin\zeta_- + i\Omega^2(A_- D_+ - B_- C_+)\sin\zeta_+\right] \\
c &= \frac{4\kappa\Omega e^{-iq^+L}}{\Gamma}\left[i(E+\sigma h)(D_+\cos\frac{\zeta_+}{2} + iC_+\sin\frac{\zeta_+}{2})\sin\frac{\zeta_-}{2}\right. \\
&\quad \left. - \Omega(C_+\cos\frac{\zeta_+}{2} + iD_+\sin\frac{\zeta_+}{2})\cos\frac{\zeta_-}{2}\right] \\
d &= \frac{4\kappa\Delta\Omega e^{iq^-L}}{\Gamma} i\left[B_-\cos\frac{\zeta_+}{2} - iA_-\sin\frac{\zeta_+}{2}\right]\sin\frac{\zeta_-}{2}
\end{aligned} \tag{4.5}$$

The probability current is obtained from $j = \Re(\psi^* \frac{\hbar}{im}\nabla\psi)$ and requiring conservation of probability. For the four different processes we then find probabilities given by $A = \frac{q^-}{q^+}|a|^2$, $B = |b|^2$, $C = |c|^2$ and $D = \frac{q^-}{q^+}|d|^2$.

4.2.1 Energy dependence

To understand the results in the coming sections it is important to understand the energy dependence of the transport coefficients. The energy enters in the expressions for A, B, C and D only through $\zeta_\pm$ (which depends on $k_{\sigma\pm}$) and Ω. In all these expressions the energy is found through terms which have the form $E + \sigma h$. This means that the Zeeman splitting of the quasiparticle states only gives a translation in energy compared to the same junction with a normal superconductor. The energy shifting has magnitude σh. An incoming particle with spin up will then have probabilities that are shifted in negative energy direction corresponding to the lowering of the energy gap ($\Delta - h$). Similarly an incoming particle with spin down will have probabilities that are shifted in the positive energy direction corresponding to the increase in the energy gap ($\Delta + h$). A plot of the coefficients for some values of Z is given in Fig. 4.3.

All coefficients oscillate with a frequency that depends on energy and the width of the superconducting film. The higher the barrier potential is the more dominant is the normal reflection coefficient. In the tunneling limit ($Z = 100$) it is the only non-zero coefficient in the plot. If we were to examine the coefficients with a higher accuracy there would however be small peaks in the A, C and D coefficients and a corresponding drop in the B coefficient. This corresponds to the peak observed

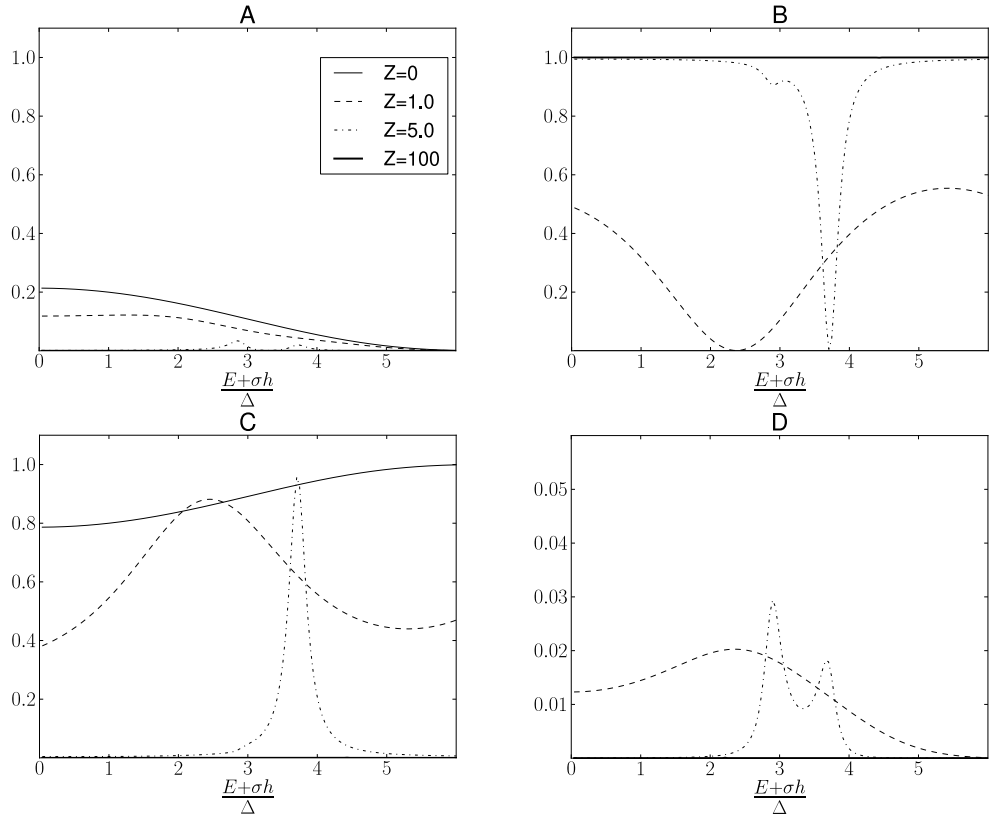

Figure 4.3: Plot of the transmission and reflection coefficients as a function of energy. The energy scale is shifted with σh compared to the same junction with a normal superconductor. The energy scale for spin up electrons is given by $\sigma = 1$ and for spin down electrons by $\sigma = -1$. In this plot we have chosen $\kappa = 1$, $\frac{\Delta}{E_F} = 10^{-3}$ and $k_F L = 10^3$ (corresponding to $\frac{L}{\xi} = 0.5$).

in C at $Z = 5.0$ and the corresponding large drop in B. In the tunneling limit these effects are small and have no consequenses for the charge transport, but will be important for the polarization of the spin current as we will se in section 4.3.2.

It is also observed that transmission as a hole (called crossed Andreev reflection for subgap energies) is a small effect compared to transmission as an electron (called elastic cotunneling for subgap energies) for low barrier strengths. At high barrier strengths they are comparable.

4.2.2 Charge conductance

There are two methods to compute the charge conductance of the three-layer system we are investigating. Which one to use depends on the external potentials in the system. The first possible choice is to put a voltage eV on the left metal and ground the superconductor and the right metal [24]. This is the simplest setup and we get a differential charge conductance proportional to $1+A-B$ in the left metal and $C-D$ in the right metal. Since probability conservation requires $A+B+C+D=1$ these

two expressions can not be equal, unless $A = -D$ which would be non-physical. As a result of this the current of the system will not be conserved in this setup. The current found in each metal will be given by

$$I_L \propto \int_{-\infty}^{\infty} dE[f_0(E - eV) - f_0(E)][1 + A(E) - B(E)]$$
$$I_R \propto \int_{-\infty}^{\infty} dE[f_0(E - eV) - f_0(E)][C(E) - D(E)] \tag{4.6}$$

Often charge conservation is one of the properties we are interested in. When looking at charge transport it is therefore common to put a voltage of $+\frac{eV}{2}$ on the left side metal and a voltage $-\frac{eV}{2}$ on the right side metal and ground the superconductor [25, 26]. This means that an electron is injected from the left side, and a hole from the right side. Following this approach will guarantee charge conservation, and the chemical potential of the superconductor can be found self-consistently. To do this we compute the current through each of the metal/superconductor interfaces and require that they should be equal. Calling the probabilities for transmission as hole and electron for $\tilde{C}$ and $\tilde{D}$ in the case of hole injection the current can be written

$$I \propto \int_{-\infty}^{\infty} dE \left[f_0\left(E - \frac{eV}{2}\right) - f_0\left(E + \frac{eV}{2}\right) \right] \left[1 + A - B + \tilde{C} - \tilde{D}\right] \tag{4.7}$$

In the zero-temperature limit the Fermi distribution function $f_0(E)$ simplifies to the step function $1 - \theta(E)$.

We are then left with two different set-ups giving different currents. Each of them involve important aspects of the transport process that should be considered. Looking at spin transport we choose to put a potential of eV on the left metal.

4.2.3 Spin conductance

When a system is spin-dependent it will often be of more interest to examine the transport of spin rather than the charge transport. Different definitions of spin current has been given in the literature. Especially when spin-flip processes are involved the definition of spin current can be ambiguous. The system we are investigating does not allow spin-flip processes. Such processes would have lead to terms in the Hamiltonian which would have prohibited the decoupling of the Bogoliubov deGennes equations. That no spin-flips occur is an important aspect and we can understand it by a quick examining of the particles that are the results of the four processes we have. Normal reflection and elastic cotunneling (transmission as electron) give electrons in the same spin band as the incoming electron. Andreev reflection and crossed Andreev reflection give a hole in the opposite spin band, which have the same effective spin as the incoming electron; that is all particles have the same effective spin as the injected particle.

Giazotto and Taddei wrote a paper on the normal metal/Zeeman splitted superconductor juntion [1]. They use the normal charge current of Eq. (4.6) when examining

the spin polarization. The same approach is used in [27]. This calculation involves the charge of the particles and thus subtracts a rightward hole current from a rightward electron current. One thus get the actual amount of total charge that is transported through the junction. On the other hand one lose information on the total spin.

Another approach is used in [28, 29]. There the spin conductance is given as $1 - A - B = C + D$. Since the transmitted electrons, C, and the transmitted holes, D, have the same effective spin, calculating the current by this approach gives the total spin that is transported in the system. Both electrons and holes (with the same spin) will then give a positive current as long as they are moving rightwards. From probability conservation we see that the total spin (in contrast to the total charge) is a conserved quantity when a potential of eV is applied to the left metal.

Our interest is for the non-local spin current, that is the spin current observed in the right metal. The two definitions for conductance will then be $G_C = C - D$ for the charge current and $G_S = C + D$ for the spin current. As the magnitude of D is small compared to C for small and intermediate values of Z the two definitions will qualitatively give the same result when calculating the spin polarization by the use of Eq. (4.8) for weak barriers. We will use the spin current throughout this text.

Of great importance to the field of spintronics is the concept of a pure spin current. Pure spin currents are currents which transport spin, but no charge [30]. If we want to obtain a pure spin current we must have an equal flow of identically spin-polarized electrons and holes in the same direction giving cancellation of charge current. This would give a spin conductance which is larger than zero and a charge conductance equal to zero.

4.3 Spin current and polarization

We want to examine if it is possible to obtain a spin-polarized non-local current on the right side of our junction when an unpolarized current is injected on the left side. An unpolarized current is a current that on average has the same number of spins pointing upwards as downwards. A polarized current on the other hand will have a majority of one type of spin. In the extreme limit of a 100% spin-polarized current all spins will be pointing in the same direction.

For a general spin-resolved quantity X one can find the polarization from the formula

$$P_X = \frac{X_\uparrow - X_\downarrow}{X_\uparrow + X_\downarrow} \tag{4.8}$$

By the use of this formula one can calculate the spin polarization of both the charge current and the spin current and any other quantity one want to examine. In the following sections our focus will be on the polarization of the spin current I_σ^S.

The expression for the spin current can be obtained in the same way as for the charge currents in Eq. (4.6) and (4.7). For incoming electrons with spin σ the non-local

spin current is given by

$$I_\sigma^S \propto \int_{-\infty}^{\infty} dE[f_0(E-eV) - f_0(E)][C(E) + D(E)] \tag{4.9}$$

This current is the foundation of the plots and discussions in the following sections. A plot of I_σ^S against the bias voltage is given in Fig. 4.4.

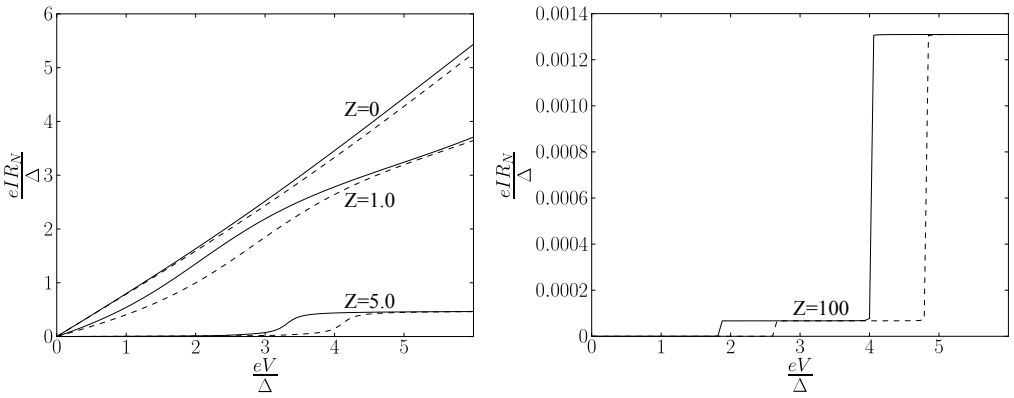

Figure 4.4: The spin current through the system vs bias voltage for different barrier strengths at $T = 0$. The solid line is for injection of spin up electrons, and the dashed line is for injection of spin down electrons. R_N is the normal state resistance. $\frac{h}{\Delta} = 0.4$, $\kappa = 1$, $\frac{\Delta}{E_F} = 10^{-3}$ and $k_F L = 10^3$.

4.3.1 Spin polarization

Figs. 4.5 and 4.6 displays the polarization of the non-local spin current against the bias voltage V at $T = 0$ for different strengths of the exchange field and several values of Z. $P(V)$ is strongly dependent on L and Z and it is an antisymmetric function of bias voltage. We will therefore only consider positive voltages. Various superconductors have a different ratio between the penetration depth and the coherence length. We restrict ourselves to type I superconductors and must have $\lambda < \xi$. To show the L-dependence of the polarization our plots are based on two superconductors requiring different thickness of the film compared to the coherence length to obtain coexistence between magnetic and superconducting correlations. Superconductors such as aluminium will require a thinner film compared to the coherence length than e.g. lead since the penetration depth is very small compared to the coherence length. The first set of plots (Fig. 4.5) have $\frac{L}{\xi} = 0.5$. This will require a penetration depth that is almost as large as the coherence length, and the superconductor will be partly a type II superconductor. The second set of plots (Fig. 4.6) have $\frac{L}{\xi} = 0.05$. Both set of plots have $L < \xi$ and thus gives coherent transport with crossed Andreev reflection and elastic cotunneling for energies below the gap energy.

The most interesting thing to notice in both sets of plots is the region with 100% polarization. This happen for a certain energy range in the tunneling limit. It is

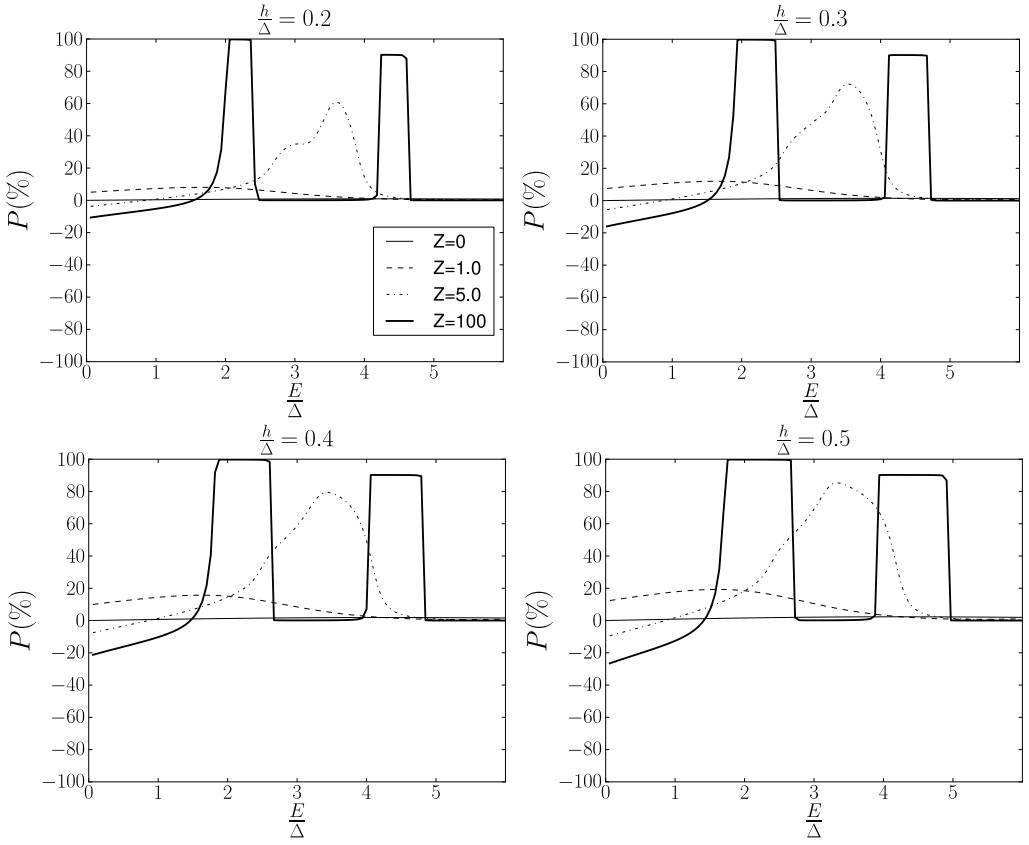

Figure 4.5: Plot of the polarization of the spin current for different barrier strengths and exchange fields when $\kappa = 1$, $\frac{\Delta}{E_F} = 10^{-3}$ and $k_F L = 10^3$ (corresponding to $\frac{L}{\xi} = 0.5$).

thus possible to obtain highly spin-polarized currents in N-S-N junctions when the superconductor is subject to a Zeeman field. In the first set of plots there is also a second peak of high polarization. We will come back to the cause of this result in section 4.3.2.

We see that the spin polarization is almost zero for the metallic interface ($Z = 0$). There is no transmission as a hole at this Z-value and the spin current is determined solely from C. Because of the gap of $2h$ between the spin up and spin down band the polarization is determined from $C(E + h)$ for spin up and $C(E - h)$ for spin down. In Fig. 4.3 we see that C varies slowly at $Z = 0$, and the difference between the C-coefficient at the two energies will be small. Then the magnitude of the difference between the spin current transported by incoming spin up and spin down electrons will be small, leading to a very low polarization. This small difference between the spin-dependent currents is easily observed in Fig. 4.4.

As the barrier potential is increased the maximum achievable polarization increases. This is caused by a larger variation in C than we had for $Z = 0$. Since the contribution of C dominates over the contribution of D when Z is not to high this will cause a larger difference between the spin up and spin down currents. The maximum polarization is where we find the largest difference between the curves in Fig. 4.4.

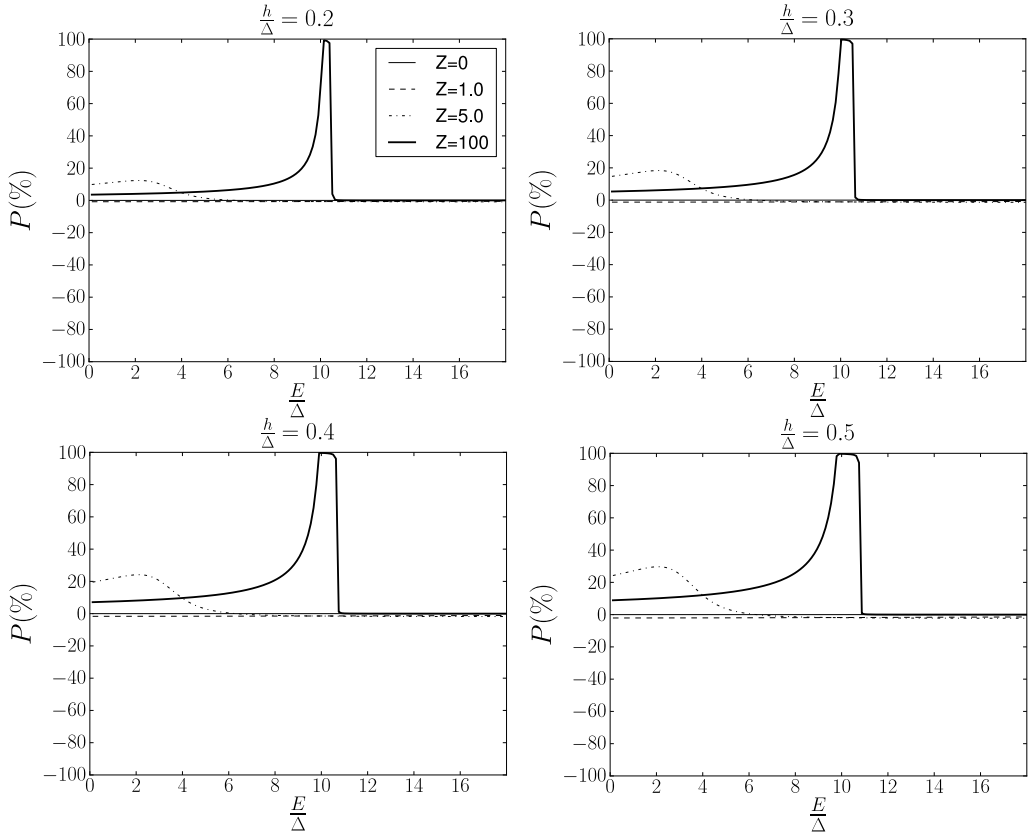

Figure 4.6: Plot of the polarization of the spin current for different barrier strengths and exchange fields when $\kappa = 1$, $\frac{\Delta}{E_F} = 10^{-3}$ and $k_F L = 100$ (corresponding to $\frac{L}{\xi} = 0.05$).

For the highest Z-values there is a transition between negative and positive polarization in Fig. 4.5. This behaviour is nontrivial and is difficult to explain completely. As we see in Fig. 4.7 the spin down current dominates up to $\frac{eV}{\Delta} \approx 1.46$. At this point the spin up current starts to increase much faster and passes the spin down current, causing the switch in the sign of the polarization. In Fig. 4.4 it can be seen that the spin down current get this same fast increase at an energy that is $2h$ larger (which is explained by the energy splitting of $2h$). The cause of this sudden increase will be explained when examining the limiting values of C and D for large Z-values.

Both set of plots show the behaviour of the polarization for increasing exchange field, h. The most important effect of increasing h is to increase the width of the region of full polarization in the tunneling limit. This width is $2h$. Another effect taking place at larger exchange fields is the enhancement of the maximum achievable polarization for low and intermediate barrier strengths. Most apparent in our plots is the $Z = 5.0$ curve where the polarization increases from about 60% for $\frac{h}{\Delta} = 0.2$ to over 80% for $\frac{h}{\Delta} = 0.5$. As a consequence of this increase the voltage interval of large polarization becomes wider.

When no voltage is applied there will be no current in the system, and naturally no

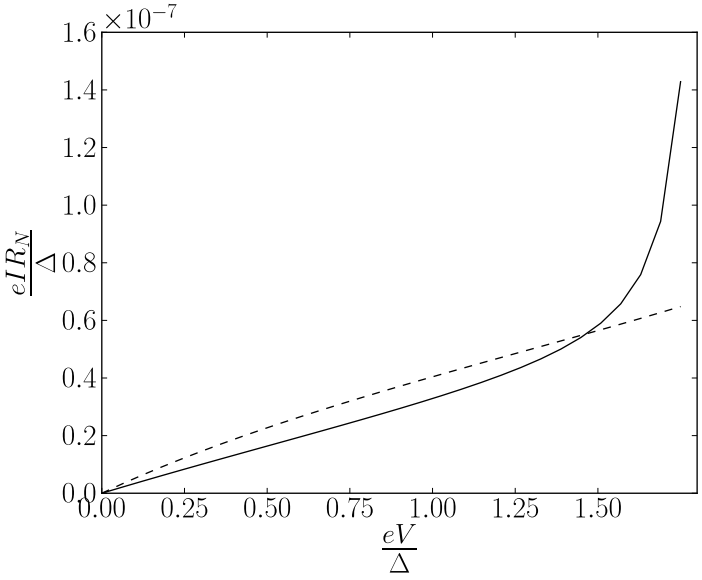

Figure 4.7: A closer look at Fig. 4.4 for $Z = 100$ at small voltages. The spin down current dominates until $\frac{eV}{\Delta} \approx 1.46$ where the spin up current become larger. This gives a switch between negative and positive polarization.

spin polarization. However, we see from the plots that there is a jump to an initial polarization P_0 taking place when a small voltage is applied. The polarization is thus discontinous at $eV = 0$. Since the only effect of a negative voltage will be to switch the sides at which holes and electrons are injected, the current and the polarization will be antisymmetric functions of eV. Then there will be a discontinuity of $2P_0$ between the positive and negative side of the zero volage point. This was not the case for the N-ZS system where there was a continious change in the spin polarization across $eV = 0$ [1]. In Fig. 4.5 P_0 is positive for small barrier strengths and then become increasingly more negative when the barrier strength increases. In the case of the thinner superconducting film in Fig. 4.6 P_0 is negative for low Z-values and positive for high Z-values. It is also observed that the absolute value of P_0 increases with increasing exchange field. From this we can clearly deduce that the initial polarization depends on barrier strength, the width of the superconductor and the exchange field in some nontrivial manner. An analytic expression is to complicated to gain much information.

From the plots for $k_F L = 1000$ it may seem as if there are more regions with negative polarization then those at low voltages. This is not the case, but is caused by the the thickness of the lines. At large voltages the polarization goes to zero in all cases. In the case of $k_F L = 100$ the polarization is on the other hand negative in more cases. For $Z = 1.0$ the polarization is negative for all energies given in the plot, and the $Z = 5.0$ curve gets negative for the largest energies.

Some other differences are observed in Fig. 4.6 compared to Fig. 4.5. The maximum polarization is much lower for barrier potentials that is well below the tunneling limit. We also find these maxima at a lower voltage, which is the opposite of what

we observe for the tunneling case where a much larger voltage is needed to achieve full polarization. Apart from that the qualitative behaviour is much the same as for the thicker film. The full polarized current is achieved at a bias voltage about 5 times larger than in the case of the thicker film, but the width of the peak is still $2h$. The reason for this is that the oscillations of the probabilities for the transport processes are strongly dependent on the width of the film. Small L-vaules give very slow oscillations which will delay the appearance of the peak. There will be a second region with a peak in the polarization as we had for $k_F L = 1000$. It is not observed in these plots, but will enter at an energy that is far to large to be considered in this system (about 51 eV). At such large energies the energy term in the denominator of C and D will be large, and the peak will be low.

4.3.2 Tunneling limit

To understand the polarization results obtained in the tunneling limit ($Z = 100$) we must examine the behaviour of the transport coefficients in the high Z limit. From Fig. 4.3 we see that the normal reflection coefficient, B, is dominating. This is as we would expect from classical physics where reflection is the only possible process when the barrier is higher than the energy. All other coefficients are zero to first order. Since normal reflection give neither spin nor charge transport both the spin and the charge current will be zero. Eq. (4.10) shows that the corrections are proportional to Z^{-4} and will give no notable contributions for most energies. Even though this contribution is really small for high Z-values a weak current will flow. This current will give rise to the polarization observed in the plots. And since the polarization is the percentage difference between the spin up current and the spin down current compared to the total spin current (and do not depend on the magnitude of the current) the current need not be strong to give high polarization.

The limiting values for the transport coefficients are given by

$$\begin{aligned} A &= \frac{16\Delta^2 \cos^2\frac{\zeta_-}{2}\sin^2\frac{\zeta_-}{2}}{((E+\sigma h)^2-\Delta^2)Z^4(\cos\zeta_- - \cos\zeta_+)^2} \\ B &= 1 - A - C - D \\ C &= \frac{16(\Omega\cos\frac{\zeta_-}{2}\sin\frac{\zeta_+}{2} - (E+\sigma h)\cos\frac{\zeta_+}{2}\sin\frac{\zeta_-}{2})^2}{((E+\sigma h)^2-\Delta^2)Z^4(\cos\zeta_- - \cos\zeta_+)^2} \\ D &= \frac{16\Delta^2 \cos^2\frac{\zeta_+}{2}\sin^2\frac{\zeta_-}{2}}{((E+\sigma h)^2-\Delta^2)Z^4(\cos\zeta_- - \cos\zeta_+)^2} \end{aligned} \tag{4.10}$$

We can understand the reasons for the regions with full and high polarization by examining the denominator in the expressions of C and D given in Eq. (4.10). The expression $(\cos\zeta_- - \cos\zeta_+)^2$ in the denominator is plotted in Fig. 4.8. It is a function of energy that oscillates with periodic points of zero.

If we compare the first zero point for spin up in Fig. 4.8 with the start of the full polarization region in Fig. 4.5 we find a correspondence. Similarily the end of the

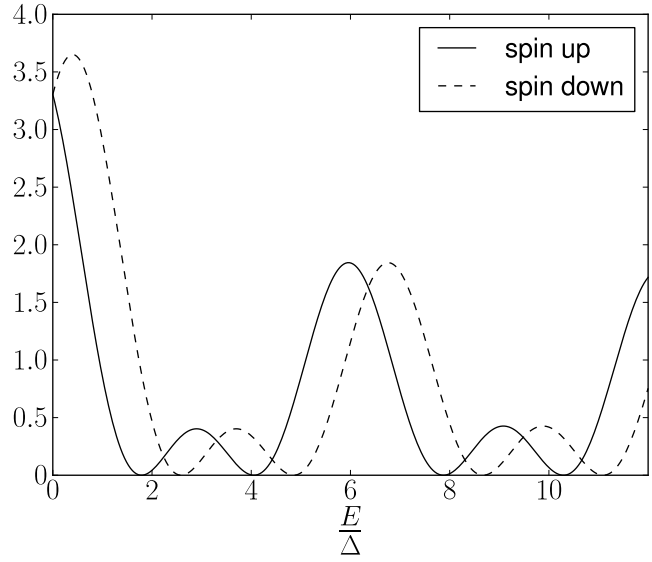

Figure 4.8: The oscillating part of the denominator of C and D in the high barrier limit when $\frac{\Delta}{E_F} = 10^{-3}$, $k_F L = 1000$ and $\frac{h}{\Delta} = 0.4$.

full polarization region correspond to the first zero point of the spin down curve. To get a better understanding of the spin current we want to find an expression for these zero points. By using trigonometric rules for addition and subtraction of angles the oscillationg part of the denominator can be rewritten as

$$\cos\zeta_- - \cos\zeta_+ = 2\sin(k_+ L)\sin(k_- L) \tag{4.11}$$

If the denominator should be zero either $\sin(k_+ L)$ or $\sin(k_- L)$ must be zero. Both equations give the same requirement

$$(E + \sigma h) = \sqrt{E_F^2 \left(\left(\frac{n\pi}{k_F L} \right)^2 - 1 \right)^2 + \Delta^2} \tag{4.12}$$

where n is a whole number. For $\kappa = 1$, $\frac{\Delta}{E_F} = 10^{-3}$ and $k_F L = 1000$ the smallest positive point is given by $n = 318$ with the value $\frac{E+\sigma h}{\Delta} \approx 2.19$, and the next by $\frac{E+\sigma h}{\Delta} \approx 4.45$. That the denominator is zero means that there is a divergence and C and D will become larger than 1. What we must remember is that this is not an exact result. If we include the next term in the high Z-limit the denominator reads $(\cos\zeta_- - \cos\zeta_+ + \frac{4}{Z}\sin\zeta_+)^2$ which would take care of the divergence, but still have near zero points.

At these points the expression for the non-local spin conductance $C + D$ suddenly increases fast. This in return will give a many-doubled value for the spin current. Since the probabilities for the spin down transmission processes are shifted by $2h$ realtive to the spin up probabilities this increase in spin current will also be shifted by the same amount, thus taking place at an energy $E + 2h$. The spin up current sets in at

$$eV_+ = \sqrt{E_F^2 \left(\left(\frac{n\pi}{k_F L} \right)^2 - 1 \right)^2 + \Delta^2} - h \tag{4.13}$$

while the spin down current starts at an energy

$$eV_- = \sqrt{E_F^2 \left(\left(\frac{n\pi}{k_F L} \right)^2 - 1 \right)^2 + \Delta^2} + h \tag{4.14}$$

Over a short energy interval around eV_+ the spin up current increases from $\sim 10^{-7}$ to $\sim 10^{-4}$, while the spin down current remains at $\sim 10^{-7}$. An increase in three orders of magnitude results in an almost fully polaraized current as we see in Fig. 4.5. At the energy $eV_- = eV_+ + 2h$ the spin down current undergoes the same increase and the polarization falls back to zero. There will thus be full polarization between the energies $\frac{eV_+}{\Delta} = 1.79$ and $\frac{eV_-}{\Delta} = 2.59$ when $\kappa = 1$, $\frac{\Delta}{E_F} = 10^{-3}$, $k_F L = 1000$ and $\frac{h}{\Delta} = 0.4$.

Further zero points can be found from the requirements. The common denominator of C and D (in the high Z limit) also includes a factor $(E + \sigma h)^2 - \Delta^2$. This will reduce the maximum value obtainable by $C + D$ and give a smaller increase in the spin current than what was observed at the first zero point. Again the spin up current will lead by $2h$ and we get a polarization of about 90.2%. More peaks will follow at higher energies, but the maximum polarization will decrease as energy increases.

For the N-ZS case full polarization was achieved in the tunneling limit for energies $|eV - \Delta| \leq h$ [1]. Here we see that we get a more complicated condition in the N-ZS-N case. It seems like the interval of full polarization depends on the geometry (the width of the superconductor compared to the coherence length), the ratio between the gap energy and the Fermi energy and on the magnitude of the Zeeman energy.

There is one other limit we will give some attention. If we switch the superconductor with a normal metal, that is $\Delta \to 0$, we get a structure with a Zeeman splitted normal metal between two normal metals. In this limit we get a remarkable result. It turns out that there still is an interval with nearly full polarization. The interval is still of width $2h$, but is translated along the energy axis compared to the case of finite Δ. As a control the same results are obtained when we calculate the transmission and reflection coefficients without ever including a superconductor. These results are remarkable in the sense that we can get a strongly spin polarized current from a system consisting of only normal metals when the applied field is small. From this we can conclude that this interval of full polarization mainly is a geometric effect. It is nevertheless interesting to use superconductors as they give the possibility of processes like crossed Andreev reflection.

Chapter 5

Magnetoresistance and spin-active interfaces

Magnetic correlations may be introduced into a superconducting hybrid structure in other ways than through a Zeeman splitting of the quasiparticle energies of the superconductor. Of much interest has been systems built up by a superconductor placed between two ferromagnetic metals. Such systems have been the subject of many papers, both theoretical and experimental (see for example refs. [25, 26, 31, 32] and [33, 34, 35] respectively). These systems show many of the same properties as the N-S-N system, but new spin-dependent behaviour is also present.

Recently an experiment [2] was carried out where the authors studied transport and resistance between two superconductors that were bridged by two parallel ferromagnetic wires, forming an S-F-F-S junction. Surprisingly the experiment showed that the resistance of the junction had a re-entrant behaviour as a function of temperature; that is upon cooling the junction below the critical temperature the resistance switched from being larger in the parallel alignment to being larger in the antiparallel alignment. The article presents a possible explanation in terms of spin-active interfaces where the particles feel different barrier potentials and acquire different phases depending on their spin.

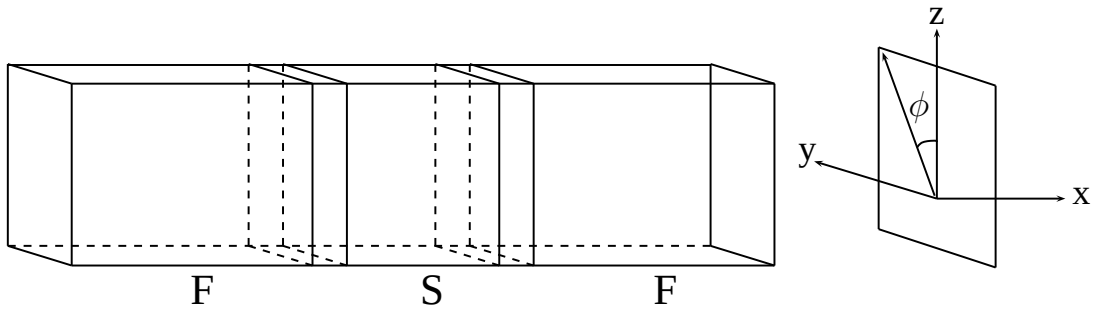

Figure 5.1: A superconducting film of width less than the penetration depth is placed between to semi-infinite ferromagnets. The potential at the interfaces is spin-dependent with a barrier moment in the yz-plane.

This motivates the second system we will examine in this thesis. The set-up is the usual one with a thin superconducting film placed between two ferromagnetic metals, that can be in either a parallel or an antiparallel alignment. In addition the F-S interfaces are made spin-active and thus responding differently to incoming spin up and down particles. Based on this we want to present a theoretical investigation of the circumstances which allow for an inverse spin-valve effect; that is a transition from postitive to negative magnetoresistance. Note that the setup in this text (see Fig. 5.1) differ a little bit from the setup in [2]. For simplicity we use a one dimensional transport model, while they use two dimensions. This will have some impact upon the magnetoresistance (MR), but it will still be possible to investigate the transition between positive and negative MR.

The magnetoresistance is defined by

$$MR = \frac{R_{AP} - R_P}{R_P} \tag{5.1}$$

where R_P and R_{AP} are the resistances in the parallel and antiparallel alignments respectively.

5.1 Bogoliubov deGennes equations

As for the N-ZS-N system the starting point will be to find the Bogoliubov deGennes (BdG) equations for the system. They can be solved to find the wave functions in the ferromagnetic and the superconducting regions respectively. We will start by expressing the Hamilton functions of the different parts by use of second quantization in momentum space. From these Hamiltonians it is the easy to find the real space version from which we derive the BdG equations.

5.1.1 Second quantized form of Hamilton functions

The superconductor is a normal BCS superconductor with a Hamilton function of the same form as (2.1). Performing a mean-field approximation along the same lines as in section 3.2 we can write

$$H_{SC} = \sum_{\mathbf{k}\sigma} \varepsilon_{\mathbf{k}} c^\dagger_{\mathbf{k}\sigma} c_{\mathbf{k}\sigma} - \sum_{\mathbf{k}\sigma\sigma'} \left[\Delta^\dagger_{\mathbf{k}\sigma\sigma'} c_{-\mathbf{k}\sigma'} c_{\mathbf{k}\sigma} + \Delta_{\mathbf{k}\sigma\sigma'} \left(c^\dagger_{\mathbf{k}\sigma} c^\dagger_{-\mathbf{k}\sigma'} - b^\dagger_{\mathbf{k}\sigma\sigma'} \right) \right] \tag{5.2}$$

Solving this give energies $E^2_{\mathbf{k}} = \left(\frac{k^2_\pm}{2m} - \mu \right)^2 + \Delta^2$ with corresponding wave vectors

$$k_\pm = \sqrt{2m(\mu \pm \sqrt{E^2 - \Delta^2})} \tag{5.3}$$

and coherence factors $u^2 = 1 - v^2 = \frac{1}{2}\left(1 + \frac{\sqrt{E^2-\Delta^2}}{E}\right)$.

The ferromagnets will have a Hamiltonian with an interaction between the spins of the individual electrons. After performing a mean-field approximation on the spin operators the ferromagnetic part of the total Hamilton function can be written as

$$H_{FM} = \sum_{\mathbf{k}\sigma} \varepsilon_{\mathbf{k}} c^\dagger_{\mathbf{k}\sigma} c_{\mathbf{k}\sigma} - \rho \sum_{\mathbf{k}\sigma\sigma'} c^\dagger_{\mathbf{k}\sigma} (\mathbf{h}\cdot\boldsymbol{\sigma})_{\sigma\sigma'} c_{\mathbf{k}\sigma'} \tag{5.4}$$

where $\mathbf{h}$ is the vector describing the magnetic exchange energy and $\boldsymbol{\sigma} = (\sigma_x, \sigma_y, \sigma_z)$ is the vector of Pauli matrices. $\rho = \pm 1$ when the polarization of the ferromagnet is in the $\pm z$-direction respectively. In this Hamiltonian we have neglected constant energy terms, as the energy can be renormalized. In our system we limit ourselves to ferromagnets polarized in the z-direction. That means we can write $\mathbf{h} = (0, 0, \pm h)$ which simplifies (5.4)

$$H_{FM} = \sum_{\mathbf{k}\sigma} (\varepsilon_{\mathbf{k}} - \rho\sigma h) c^\dagger_{\mathbf{k}\sigma} c_{\mathbf{k}\sigma} \tag{5.5}$$

The electron energies will then be $E_{\mathbf{q}} = \left(\frac{q_e^2}{2m} - \mu\right) - \rho\sigma h$ while the hole energies are $E_{\mathbf{q}} = -\left(\frac{q_h^2}{2m} - \mu\right) + \rho\sigma h$. The corresponding wave vectors are

$$q^\sigma_{\substack{e\\h}} = \sqrt{2m\left(\mu + \rho\sigma h \pm E\right)} \tag{5.6}$$

where the $+$ sign refer to the electron wave vectors and the $-$ sign to the hole wave vectors.

5.1.2 Deriving BdG equations

When deriving the BdG equations we will work in the real space domain. The real space Hamiltonian will be based on the second quantized forms in Eqs. (5.2) and (5.4). An advantage of the real space form of the Hamiltonian is that it is easy to include terms that is restricted to one part of space. We can thus include the interface potentials as well as write both the superconducting and ferromagnetic parts in one Hamilton function. We get

$$\begin{aligned}
\hat{H}_{\sigma\sigma'} &= \int \mathrm{d}x\, \psi^\dagger_\sigma \left[-\frac{\nabla^2}{2m} - \mu(x) + V_0(\delta(x) + \delta(x-L)) \right] \psi_\sigma(x,t) \\
&+ \frac{1}{2} \iint \mathrm{d}x\mathrm{d}x' \left[\Delta^\dagger_{\sigma\sigma'}(x,x') \psi_{\sigma'}(x',t) \psi_\sigma(x,t) \right. \\
&+ \left. \Delta_{\sigma\sigma'}(x,x') \psi^\dagger_\sigma(x,t) \psi^\dagger_{\sigma'}(x',t) \right] \theta(x)\theta(L-x) \\
&- \int \mathrm{d}x\, \psi^\dagger_\sigma(x,t) ((\mathbf{V_M} + \mathbf{h})\cdot\boldsymbol{\sigma}) \psi_{\sigma'}(x,t)
\end{aligned} \tag{5.7}$$

Constant terms have been taken care of by a renormalization. $\mathbf{V_M}$ is the magnetic exchange field vector of the magnetic barrier potential. When this potential is limited to the yz-plane we can write

$$\mathbf{V_M} = \big(0, V_{1y}\delta(x) + V_{2y}\delta(x-L), V_{1z}\delta(x) + V_{2z}\delta(x-L)\big) \tag{5.8}$$

while the ferromagnetic exchange field is

$$\mathbf{h} = \big(0, 0, h[\theta(-x) + \rho\theta(x)]\big) \tag{5.9}$$

$\rho = 1$ when the right ferromagnet is in parallel alignment with the left one and $\rho = -1$ when the alignment is antiparallel.

The magnetic moment at the interface constitutes a spin-dependent potential with $V_{iy} = \gamma V_0 \sin\phi_i$ and $V_{iz} = \gamma V_0 \cos\phi_i$ where $i = 1, 2$ gives the potential at the first and second F-S interface respectively. The angle ϕ is shown in Fig. 5.1. A more general barrier potential would include an x-component, but that would have gone beyond the scope of this text. For simplicity we will let the two barrier potentials be aligned giving $\phi_1 = \phi_2$. V_0 is the non-magnetic potential, while $\gamma = \frac{[\mathbf{V_M}]}{V_0}$ gives the ratio between the magnitude of the magnetic and the non-magnetic potential.

The complete Hamilton operator is given by $\hat{H} = \sum_{\sigma\sigma'} \hat{H}_{\sigma\sigma'}$, while the field operators have the following time dependence $\psi(x,t) = e^{i\hat{H}t}\psi(x)e^{-i\hat{H}t}$. The field operators must then obey the Heisenberg equations of motion. Using the anticommutator relation between fermionic operators $\big\{\psi^\dagger_\sigma(x,t), \psi_{\sigma'}(x',t)\big\} = \delta_{\sigma\sigma'}\delta(x-x')$ we get the following expressions

$$\begin{aligned} & i\partial_t\psi_\alpha(x,t) = \Big[\psi_\alpha(x,t), \hat{H}\Big] \\ = & \sum_{\sigma'} \int \Big(\delta(x-x')\hat{H}^0_{\alpha\sigma'}(x',\hat{p})\psi_{\sigma'}(x',t) + \Delta_{\alpha\sigma'}(x,x')\psi^\dagger_{\sigma'}(x',t)\Big) \end{aligned} \tag{5.10}$$

and correspondingly

$$\begin{aligned} & i\partial_t\psi^\dagger_\alpha(x,t) = \Big[\psi^\dagger_\alpha(x,t), \hat{H}\Big] \\ = & \sum_{\sigma'} \int \Big(\delta(x-x')[-\hat{H}^0(x',-\hat{p})]^{\mathrm{T}}_{\alpha\sigma'}\psi^\dagger_{\sigma'}(x',t) + \Delta^\dagger_{\alpha\sigma'}(x,x')\psi_{\sigma'}(x',t)\Big) \end{aligned} \tag{5.11}$$

where $\hat{H}^0_{\sigma\sigma'} = -\frac{\nabla^2}{2m} - \mu(x) + V_0(\delta(x) + \delta(x-L)) - [\mathbf{V_M}\boldsymbol{\sigma}]_{\sigma\sigma'}$. We introduce $\Psi(x,t) = \Big[\psi_\uparrow(x,t), \psi_\downarrow(x,t), \psi^\dagger_\uparrow(x,t), \psi^\dagger_\downarrow(x,t)\Big]^{\mathrm{T}}$ as basis, and assume an energy dependence of the field operators given by $\Psi(x,t) = \Psi(x)e^{-iEt}$. Eqs. (5.10) and (5.11) can then be written more compactly

$$E\Psi(x) = \int \mathrm{d}x' \mathcal{H}(x,x')\Psi(x') \tag{5.12}$$

where

$$\mathcal{H}(x,x') = \begin{pmatrix} \hat{H}^0(x',p)\delta_{xx'} & \hat{\boldsymbol{\Delta}}(x,x') \\ \hat{\boldsymbol{\Delta}}^\dagger(x,x') & [-\hat{H}^0(x',-p)]^{\mathrm{T}}\delta_{xx'} \end{pmatrix} \tag{5.13}$$

In this expression $\hat{\mathbf{\Delta}}(x,x') = i\sigma_y\Delta(x,x')$ and $\delta_{xx'} = \delta(x-x')$.

We consider plane wave solutions of $\Psi(x)$ and divide out fast oscillations as in [36]. For simplicity we will not find the spatial dependence of the order parameter near the interfaces, but perform the step function approximation $\Delta(x) = \theta(x)\theta(L-x)\Delta$. This means that we assume a constant gap throughout the superconductor at a given temperature. The Bogoliubov deGennes equations will then be

$$\hat{H}\Psi(x) = E\Psi(x) \tag{5.14}$$

with

$$\hat{H} = \begin{pmatrix} H_0 - h(x) + V_\uparrow(x) & iV_y(x) & 0 & \Delta(x) \\ -iV_y(x) & H_0 + h(x) + V_\downarrow(x) & -\Delta(x) & 0 \\ 0 & -\Delta(x) & -H_0 + h(x) - V_\uparrow(x) & iV_y(x) \\ \Delta(x) & 0 & -iV_y(x) & -H_0 - h(x) - V_\downarrow(x) \end{pmatrix} \tag{5.15}$$

where $H_0 = -\frac{\nabla^2}{2m} - \mu(x)$ and $V_\sigma = V_0 - \sigma V_z$.

5.1.3 Transport coefficients

Solving Eq. (5.14) we get the wave functions in the left ferromagnet

$$\begin{aligned} \psi_{FL}(x) &= \begin{pmatrix} s^\uparrow \\ 0 \\ 0 \\ 0 \end{pmatrix} e^{iq_e^\uparrow x} + \begin{pmatrix} 0 \\ s^\downarrow \\ 0 \\ 0 \end{pmatrix} e^{iq_e^\downarrow x} + r_e^\uparrow \begin{pmatrix} 1 \\ 0 \\ 0 \\ 0 \end{pmatrix} e^{-iq_e^\uparrow} \\ &+ r_e^\downarrow \begin{pmatrix} 0 \\ 1 \\ 0 \\ 0 \end{pmatrix} e^{-iq_e^\downarrow} + r_h^\uparrow \begin{pmatrix} 0 \\ 0 \\ 1 \\ 0 \end{pmatrix} e^{iq_h^\uparrow} + r_h^\downarrow \begin{pmatrix} 0 \\ 0 \\ 0 \\ 1 \end{pmatrix} e^{iq_h^\downarrow} \end{aligned} \tag{5.16}$$

the superconductor

$$\begin{aligned} \psi_S(x) &= \begin{pmatrix} u \\ 0 \\ 0 \\ v \end{pmatrix} \left(ae^{ik_+x} + be^{-ik_+x}\right) + \begin{pmatrix} 0 \\ u \\ -v \\ 0 \end{pmatrix} \left(ce^{ik_+x} + de^{-ik_+x}\right) \\ &+ \begin{pmatrix} 0 \\ -v \\ u \\ 0 \end{pmatrix} \left(ee^{ik_-x} + fe^{-ik_-x}\right) + \begin{pmatrix} v \\ 0 \\ 0 \\ u \end{pmatrix} \left(ge^{ik_-x} + he^{-ik_-x}\right) \end{aligned} \tag{5.17}$$

and the right ferromagnet

$$\psi_{FR}(x) = t_e^{\uparrow}\begin{pmatrix}1\\0\\0\\0\end{pmatrix}e^{iq_e^{\uparrow}} + t_e^{\downarrow}\begin{pmatrix}0\\1\\0\\0\end{pmatrix}e^{iq_e^{\downarrow}} + t_h^{\uparrow}\begin{pmatrix}0\\0\\1\\0\end{pmatrix}e^{-iq_h^{\uparrow}} + t_h^{\downarrow}\begin{pmatrix}0\\0\\0\\1\end{pmatrix}e^{-iq_h^{\downarrow}} \quad (5.18)$$

Here $\{s^{\uparrow}, s^{\downarrow}\} = \{1, 0\}$ for an incoming spin up electron and $\{s^{\uparrow}, s^{\downarrow}\} = \{0, 1\}$ for an incoming spin down electron.

The boundary conditions are still continuity of the wavefunction at the interfaces and a discontinuity of the first derivatives caused by the delta function potentials. The discontinuity conditions will however differ from the ones we had without a spin-active barrier potential. Since the magnetic moment of the barrier not necessarily is aligned along the z-direction we will get off-diagonal elements in the boundary conditions resulting in spin mixing.

$$\psi'(0^+) - \psi'(0^-) = 2mV_0\left[\mathbb{I} - \gamma\begin{pmatrix}\cos\phi & -i\sin\phi & 0 & 0\\ i\sin\phi & -\cos\phi & 0 & 0\\ 0 & 0 & \cos\phi & i\sin\phi\\ 0 & 0 & -i\sin\phi & -\cos\phi\end{pmatrix}\right]\psi(0) \quad (5.19)$$

$$\psi'(L^+) - \psi'(L^-) = 2mV_0\left[\mathbb{I} - \gamma\begin{pmatrix}\cos\phi & -i\sin\phi & 0 & 0\\ i\sin\phi & -\cos\phi & 0 & 0\\ 0 & 0 & \cos\phi & i\sin\phi\\ 0 & 0 & -i\sin\phi & -\cos\phi\end{pmatrix}\right]\psi(L) \quad (5.20)$$

where $\mathbb{I}$ is the $4x4$ identity matrix.

From these boundary conditions we get a linear system of equations with 16 unknowns. Some simplifications can be made. The usual approximation that $k^+ \approx k^- \approx k_F$ is made wherever they appear except in exponents. The same approximation can not be made for the ferromangetic momenta since h is near the same order of magnitude as μ. However, the energy dependence is small and can be neglected such that $q_e^{\uparrow} = q_h^{\uparrow}$ and correspondingly $q_e^{\downarrow} = q_h^{\downarrow}$.

We want to investigate the sign of the magnetoresistance of the system. It is then necessary to find expression for the conductance. When we looked at the spin current in the previous chapter, we chose to put a voltage on the left side and ground the superconductor and the right side. Now we want to examine charge current, and want this current to be conserverd throughout the system. We then apply a voltage of $\frac{eV}{2}$ on the left side and a voltage $-\frac{eV}{2}$ on the right side. This corresponds to incoming electrons from the left and incoming holes from the right. As incoming particles with spin up and down give different reflection and transmission amplitudes we must then compute the four reflection and four transmission coefficients for incoming electrons and holes with spin up and spin down, resulting in 32 coefficients.

With spin-active interfaces there will be few symmetries and we can not assume that some of these coefficients will be equal. The expressions for the transport coefficients are far too complicated to give analytically, and all following results are numerical.

To find the conductance we follow the same lines as [25]. First we write down the currents that can be found through the left and the right FM-S interface respectively

$$\begin{aligned} I_L = e(\mu_L - \mu) \sum_\sigma P_\sigma [1 - R_{e^\sigma e^\uparrow} - R_{e^\sigma e^\downarrow} + R_{e^\sigma h^\uparrow} + R_{e^\sigma h^\downarrow} \\ + T_{h^\sigma h^\uparrow} + T_{h^\sigma h^\downarrow} - T_{h^\sigma e^\uparrow} - T_{h^\sigma e^\downarrow}] \end{aligned} \tag{5.21}$$

$$\begin{aligned} I_R = e(\mu - \mu_R) \sum_\sigma P_\sigma [1 - R_{h^\sigma h^\uparrow} - R_{h^\sigma h^\downarrow} + R_{h^\sigma e^\uparrow} + R_{h^\sigma e^\downarrow} \\ + T_{e^\sigma e^\uparrow} + T_{e^\sigma e^\downarrow} - T_{e^\sigma h^\uparrow} - T_{e^\sigma h^\downarrow}] \end{aligned} \tag{5.22}$$

Using that $\mu_L = \mu_R$ and that $I_L = I_R$ we find that the conductance at zero temperature can be written

$$\begin{aligned} G = G_N [P_\uparrow (1 - R_{e^\uparrow e^\uparrow} - R_{e^\uparrow e^\downarrow} + R_{e^\uparrow h^\uparrow} + R_{e^\uparrow h^\downarrow} + T_{h^\uparrow h^\uparrow} + T_{h^\uparrow h^\downarrow} - T_{h^\uparrow e^\uparrow} - T_{h^\uparrow e^\downarrow}) \\ + P_\downarrow (1 - R_{e^\downarrow e^\uparrow} - R_{e^\downarrow e^\downarrow} + R_{e^\downarrow h^\uparrow} + R_{e^\downarrow h^\downarrow} + T_{h^\downarrow h^\uparrow} + T_{h^\downarrow h^\downarrow} - T_{h^\downarrow e^\uparrow} - T_{h^\downarrow e^\downarrow})] \end{aligned} \tag{5.23}$$

where $P_\uparrow = \frac{1}{2}(1 + \frac{h}{E_F})$ and $P_\downarrow = \frac{1}{2}(1 - \frac{h}{E_F})$.

5.1.4 Temperature dependence

For finite temperatures we must take into account that the distribtuion function no longer is a step function. We need the Fermi distribution function $f_0(E)$ given by

$$f_0(E) = \frac{1}{1 + e^{\frac{E}{k_B T}}} \tag{5.24}$$

Then the current at the desired temperature can be found by integrating the conductance over energy

$$I(eV, Z, \gamma, \phi, \rho, T) = \frac{1}{e} \int_{-\infty}^{\infty} dE \left[f_0 \left(E - \frac{eV}{2} \right) - f_0 \left(E + \frac{eV}{2} \right) \right] G(E, Z, \gamma, \phi, \rho, T) \tag{5.25}$$

In order to perform this integration we need the temperature dependence of the gap parameter. The gap parameter for s-wave superconductors must be a monotonic decreasing function obeying the limiting conditions $\Delta(0) = \Delta_0$ and $\Delta(T_C) = 0$. A usual assumption is the relation [37]

$$\Delta(T) = \Delta_0 \tanh \left(1.74 \sqrt{\frac{T_C}{T} - 1} \right) \tag{5.26}$$

The temperature dependence of Δ given in Eq. (5.26) is shown in Fig. 5.2. That the energy gap gradually become smaller has important consequences for the transmission and reflection coefficients. All processes involving either Andreev reflection or crossed Andreev reflection become less likely to happen with a lower energy gap, and as $T \to T_C$ the probabilities go to 0. This is because these processes need the superconducting Cooper states which cease to exist when the superconducting state is destroyed above the critical temperature. Since conservation of probability is necessary processes involving normal reflection and transmission will then become more probable.

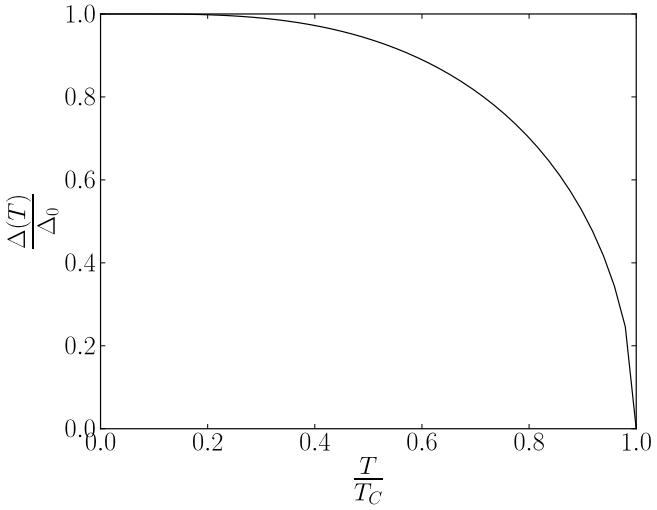

Figure 5.2: The energy gap as a function of temperature.

5.2 Magnetoresistance

All the necessary theory we need for examining the magnetoresistance is now presented. We want to find if spin-active interfaces can give a switch between positive and negative MR, and if that is possible to find the reasons for this behaviour.

5.2.1 Parameter values

The magnetoresistance depends on many different parameters, and it will be beyond the scope of this thesis to find the full dependence on all of them. We will therfore limit ourselves to certain values for some parameters. The superconductor is an s-wave superconductor where a simple and natural choice is to set $\frac{\Delta}{E_F} = 10^{-3}$. The ratio between the Fermi momenta is set to $\kappa = \frac{q_F}{k_F} = 1$. Of reasons soon to be explained we choose $Z = 0.35$, corresponding to a weakly transparent interface, in all plots (apart from Fig. 5.9) of MR as a function of temperature.

We have assumed the standard step function approximation for the gap parameter in the superconductor. Doing this we have neglected the proximity effect at the interfaces. For an exact solution we would have to find a self-consistent solution for the gap function. This would show some partial depletion of Δ_0 near the interfaces, caused by the ferromagnets. In order to justify this approximation we will only consider small voltages $\frac{eV}{\Delta_0} \ll 1$ since larger voltages would lead to a substantial accumulation of spin in the superconductor. This would suppress the gap and eventually destroy the superconducting properties. For $\frac{eV}{\Delta_0} \ll 1$ a self-consistent solution for the gap is not required [38]. The approximation will also improve for increasing thickness of the superconducting layer. As long as $L \geq 2\xi$ the approximation should be reasonable. This prevents the approximation from being good in the coherent case, that is when the width of the superconductor is less than the superconducting coherence length. A reasonable choice according to these criteria will then be $k_F L = 4000$ corresponding to $\frac{L}{\xi} = 2.0$. This value is used in all of our results, and should give reasonably good results.

We are then left with four parameters; γ giving the ratio between the magnetic and the non-magnetic barrier potential, ϕ which gives the alignment of the magnetic interface potential, h giving the strength of the exchange field in the ferromagnets, and last the temperature T. The following discussion will try to investigate how the magnetoresistance depends on these four parameters.

5.2.2 Zero temperature

At zero temperature the MR can (as in [38]) easily be evaluated by use of the conductance instead of the resistance. Then the conductance is given by the inverse of the resistance. By direct substitution in (5.1) we find that the MR is

$$MR = \frac{G_P - G_{AP}}{G_{AP}} \tag{5.27}$$

This will simplify the calculations as the zero temperature conductance can be found directly from Eq. (5.23). As a control of the calculations we let $\gamma = 0$ (that is no spin-active interfaces) and plot the conductance in the parallel and the antiparallel alignment. This reproduces the results for the simple F-S-F system given in [25] (their Z equals the half of ours). The plot is given in Fig 5.3.

As we see in Fig. 5.3 the two conductance curves have the same phase, but with largest conductance in the parallel alignment. This gives a positive magnetoresistance which is what we intuitively would expect. In the antiparallel alignment the two ferromagnets favours opposite spin. Since the two electrons of a Cooper pairs should have opposite spin, crossed Andreev reflection will be enhanced when the ferromangets have exchange fields pointing in opposite directions. Crossed Andreev reflection is however a weak effect compared to elastic cotunneling, or direct transmission, which is the process that is favoured in the parallel alignment.

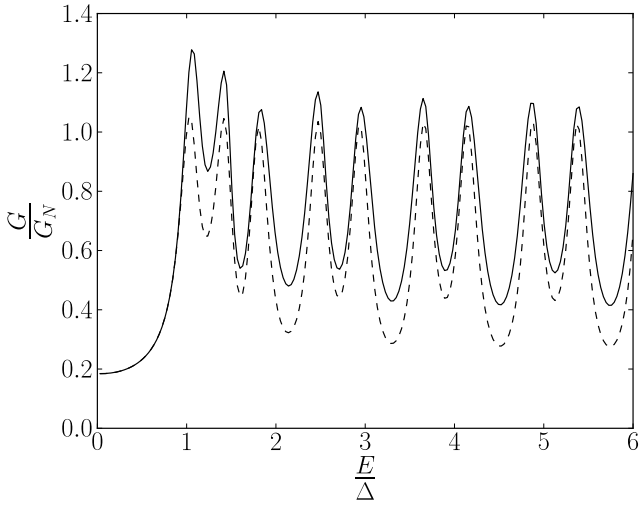

Figure 5.3: A plot of the conductance normalized by the conductance of the normal state (G_N) for $T = 0$, $\gamma = 0$, $Z = 2$, $\frac{\Delta}{E_F} = 10^{-3}$, $k_F L = 5000$ and $\frac{h}{E_F} = 0.5$. This reproduces the results of [25]. The solid line is for the parallel alignment, while the dashed line is for the antiparallel alignment.

In Figs. 5.4 and 5.5 the magnetoresistance is plotted against the non-magnetic barrier potentials for different strengths of the exchange field. In the first set of plots $\gamma = 0.1$ which give a weak magnetic potential compared to the non-magnetic potential. For the two strongest ferromagnets ($x = 0.2$ and $x = 0.5$) the MR is observed to be positive for all values of Z for both given directions of the magnetic barrier. With such strong exchange fields a magnetic barrier which is just 10% of the normal barrier will be to weak to alter the transport processes in such a degree that there will be a change in the preferred ferromagnet alignment. We observe that the magnitude of the MR is small, which means that the difference in conductance between the two alignments is small. At increasing exchange field the magnitude of the MR also increases.

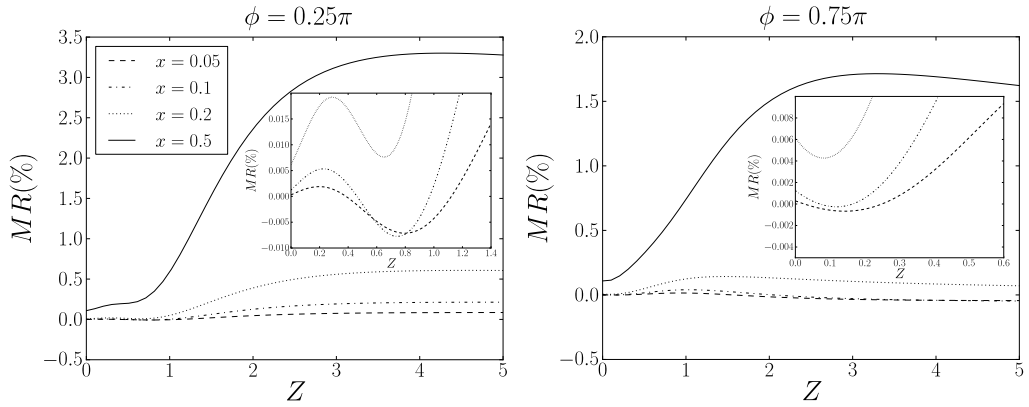

Figure 5.4: The magnetoresistance as a function of the non-magnetic barrier potential for four different exchange fields ($x = \frac{h}{E_F}$) at $T = 0$ and $\gamma = 0.1$. The inset panels give a clearer view of the sign changes for small Z.

With weaker ferromagnets we see that there is a change in sign of the MR. For $\phi = 0.25\pi$ the MR drops under zero in a small interval around $Z = 1.0$ before it again becomes positive. In this case the magnetic barrier has a positive z-component which should favour transport in the parallel alignment since the magnetic potential will be lower for spin up particles. The y-component of the barrier will however introduce an extra phase-difference. This phase-difference gives oscillations which might give negative MR. It is easier to understand the negative MR for $\phi = 0.75\pi$. The magnetic potential will have a negative z-component which reduces the total barrier for down spins, and increases the probability for spin-flip processes which in turn will increase the conductance in the AP alignment.

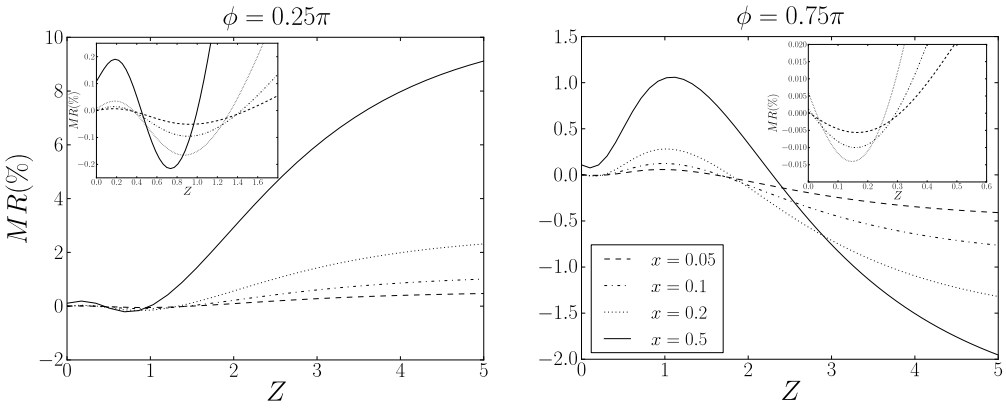

Figure 5.5: The magnetoresistance as a function of the non-magnetic barrier potential for four different exchange fields ($x = \frac{h}{E_F}$) at $T = 0$ and $\gamma = 0.5$. The inset panels give a clearer view of the sign changes for small Z.

The set of plots given in Fig. 5.5 is for $\gamma = 0.5$, that is a magnetic potential with half the strength of the non-magnetic one. A similar, but clearer, Z-dependence is found here. The region with negative MR for $\phi = 0.25\pi$ is narrower but with larger maximal negative magnitude, and now the magnetic potential is strong enough to make the MR negative for the two strongest fields. For $\phi = 0.75\pi$ we clearly see that the oscillation has nearly the opposite phase of the $\phi = 0.25\pi$ case. This can be explained by the trigonometric relation $\cos(\frac{\pi}{2} - \theta) = -\cos(\frac{\pi}{2} + \theta)$. The z-component of the barrier potential for spin up particles is thus increased in the $\phi = 0.75\pi$ case with the same amount as it decreases for $\phi = 0.25\pi$, and opposite for spin down particles. The y-component is the same for the two angles. The three weakest fields give an initial negative MR before it becomes positive, and then all curves turn negative for the largest Z-values. As the MR has a complex dependence on many parameters it is difficult to explain this behaviour, but it might be caused by the reduced dominance of elastic cotunneling compared to crossed Andreev reflection for increasing values of Z. In both sets of plots the MR will stabilize as Z is increased, and no more sign changes are observed at $T = 0$ for larger Z.

The clearest change in sign in MR as a function of Z for zero temperature is observed for large γ and large ϕ. It is thus preferrable to have a strong magnetic barrier that favours spins directed opposite to the first ferromagnet to obatin a clear change of sign in magnetoresistance as a function of Z at $T = 0$.

5.2.3 Comparison of transport coefficients

As we shall see in the magnetoresistance plots it is even more difficult to explain the behaviour for finite temperatures. To get some understanding we need to know how the transport processes for different incoming particles behave as a function of the angle and of temperature. There are too many coefficients and a too large parameter space to show all, but in Fig 5.6 we give the difference between the reflection coefficients for incoming spin up electrons in the two alignments, and corresponding plots for the transmission coefficients of incoming spin up holes. The plots are given for $\gamma = 1$ as a strong magnetic barrier most likely will give the clearest picture of the processes. The plotted coefficients are given since they are the most dominating ones (see Eq. (5.23)). Corresponding coefficients for incoming particles with spin down are very similar, but with a few important differences. The curve for normal reflection without spin flip for incoming spin down and $\phi = 0.25\pi$ is e.g. almost a reflection across the line $T = 0$ of the same process for incoming spin up with $\phi = 0.75\pi$. We have chosen to plot the difference in probability between the two alignments since curves for parallel and antiparallel alignment lies really close and would be difficult to distinguish.

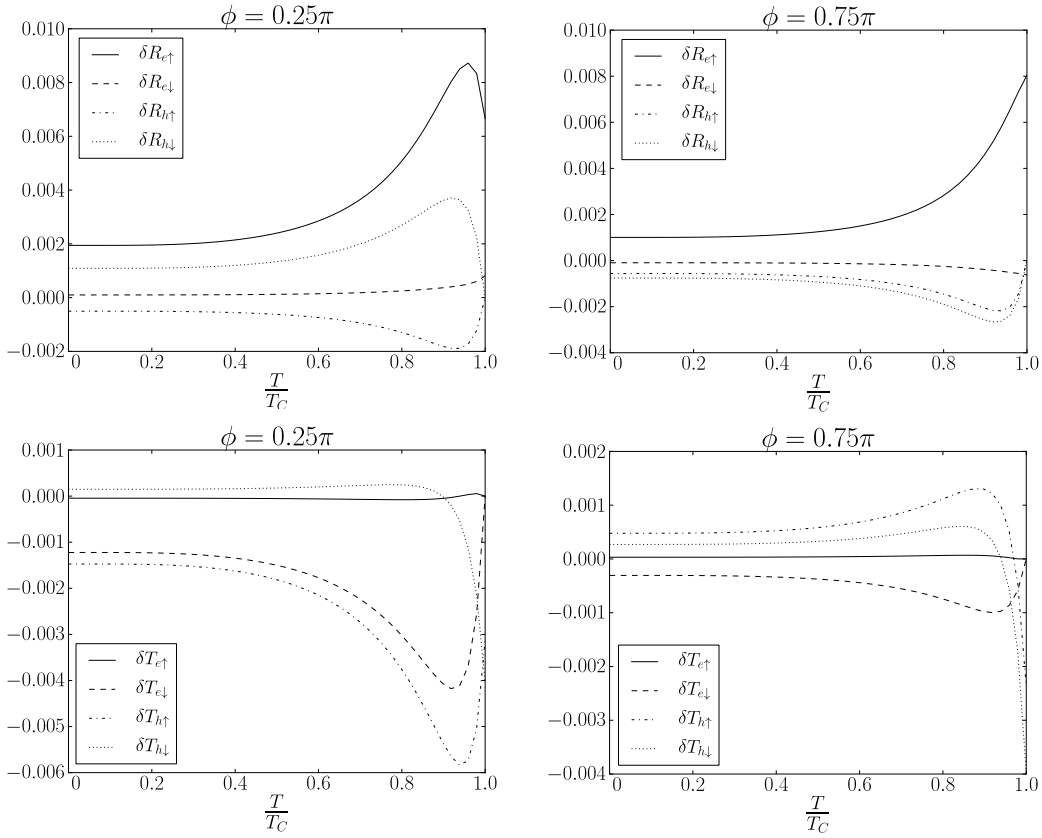

Figure 5.6: Two upper graphs: Difference between the reflection coefficients for incoming spin up electrons in the parallel and the antiparallel alignment. Two lower graphs: Difference between the transmission coefficient for incoming spin up holes in the parallel and antiparallel alignment. $Z = 0.35$, $\gamma = 1$ and $x = 0.1$.

All processes involving particle conversion (local and non-local Andreev processes) go to zero when the temperature approaches the critical temperature. Normal Andreev reflection favours parallel alignment up to an angle a little larger than $\phi = 0.5\pi$. The smaller γ is the larger is the angle needed before the antiparallel alignment is favoured. Andreev reflection without spin flip gives a negative result for all angles. The same is the result for crossed Andreev reflection with spin flip. Crossed Andreev reflection without spin flip has a very small difference between the two alignments and gives only a small contribution to the total result even though there is a change in sign for small angles. Normal reflection prefers a parallel alignment for all temperatures, and the difference increases with temperature apart from a small drop for $\phi = 0.25\pi$. With a spin flip the result is positive for small angles and negative for large angles. Normal transmission is negative for small angles and changes sign from positive to negative for large angles. Transmission with spin flip goes from positive to negative for both angles. With these results it will be easier to understand the most important aspects from Fig. 5.8.

5.2.4 Finite temperatures

First of all we give a plot of the resistance for both alignments for a weak barrier potential, the same strength of the non-magnetic and the magnetic barriers, and with the magnetic barrier along the positive z-axis. This is motivated by the experimental paper [2] on the same system, where they found a change in the sign of the magnetoresistance as a function of temperature for similar parameters.

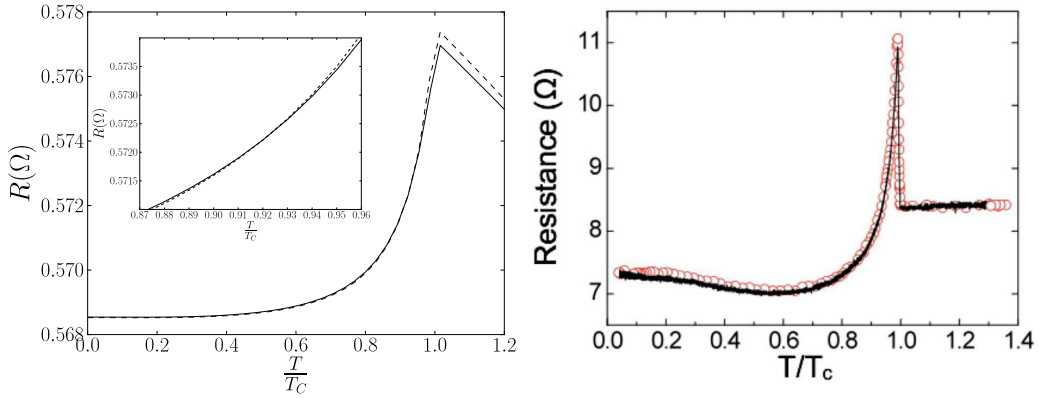

Figure 5.7: The resistance of the parallel alignment (whole line) and antiparallel alignment (dashed line) for $Z = 0.35$, $\gamma = 1.0$ and $\phi = 0$. The inset panel zooms in at the area where the antiparallel resistance becomes larger than the parallel resistance. The right plot shows the experimental results from [2].

As we see in Fig. 5.7 the curves of the two aligments follow eachother closely. For temperatures near $T = 0$ the resistance is largest in the parallel alignment, but a little above $T = 0.9T_C$ the magnetoresistance changes sign. If we compare our curves with the experimental curves the structure is much the same. There they start out at with a low resistance before it increases towards $T = T_C$ and then have a

drop when the curves leave the superconducting region. Differences we can observe compared with the experimental curves is that we miss a small drop in resistance for intermediate temperatures. This may be caused by the slightly different setup (see the start of this chapter) we use in our text, or it may be caused by some differences in parameter definitions. Another difference is found in the drop for temperatures above the critical temperature. This drop is much more abrupt in the experimental case. This is most probably explained by some numerical factor. The reason that the magnitude of the theoretical resistance is much lower than the experimental one may partly be explained by impurities in the materials which is not considered in our theoretical model.

Motivated by this we investigate the magnetoresistance for different values of γ and ϕ for $Z = 0.35$ to see how these parameters affect the sign. In Fig. 5.8 plots of the MR is given for different γ and ϕ.

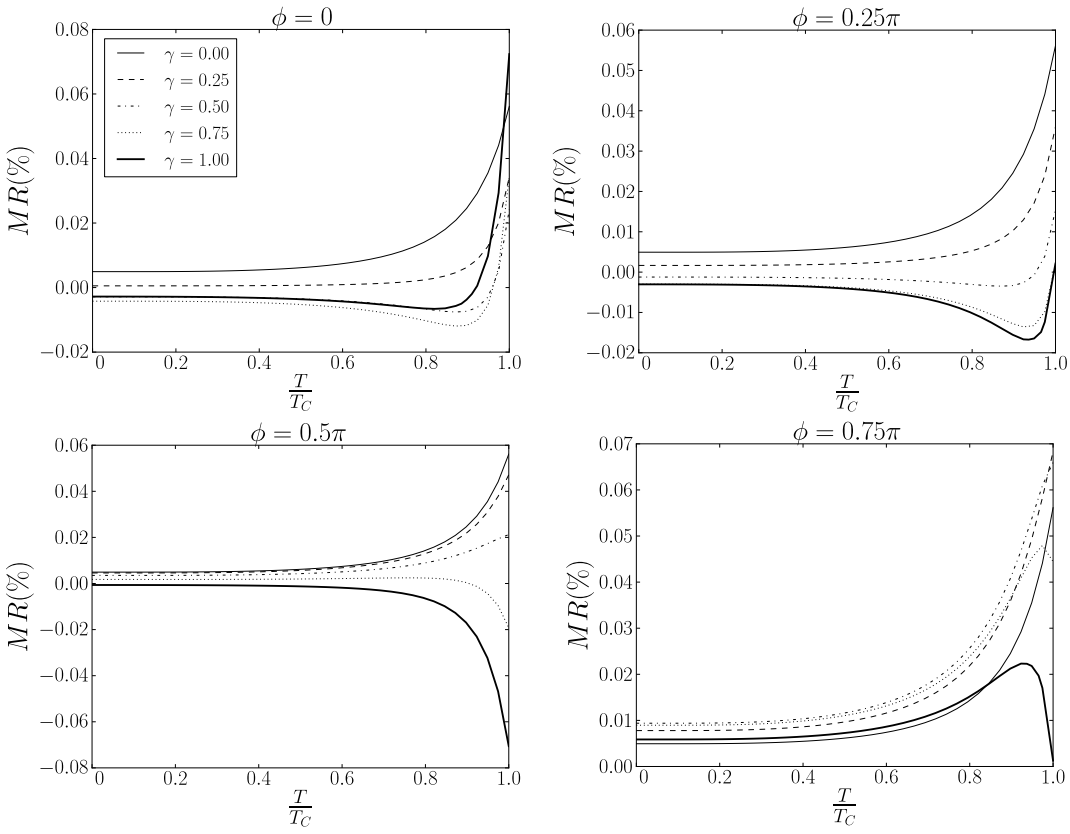

Figure 5.8: The magnetoresistance as a function of temperature for $Z = 0.35$ and different γ and ϕ. The ferromagnets considered have a strength of $x = 0.1$.

The two weakest magnetic potentials ($\gamma = 0$ and $\gamma = 0.25$) show the same structure as the resistance in Fig. 5.7. The curve is flat until it has a sudden increase towards $T = T_C$. For the three other curves we observe more interesting effects. When the angle between the magnetic barrier and the z-axis is small all three curves show a change in sign of the MR. They start out with negative MR, are relatively flat until about $T = 0.5T_C$. Then the MR decreases until a minima at about $T = 0.9T_C$ before it increases, becomes positive and follows the same trend as the

two first curves towards $T = T_C$. As the angle increases this situation changes. At $\phi = 0.5\pi$ the $\gamma = 0.5$ curve follows the $\gamma = 0$ and $\gamma = 0.25$ curves. The curves of the two strongest magnetic moments are also changed. The drop at intermediate temperatures are gone and both curves decrease towards a negative $T = T_C$ value. There is still a change in sign for the $\gamma = 0.75$ curve since it now starts out with a positive MR, but the $\gamma = 1.0$ curve now has a negative MR for all temperatures in the superconducting region. As the angle is increased even more all curves give positive MR. And when $\phi = \pi$ all curves show the behaviour in Fig. 5.7 up to the critical temperature.

It seems like the re-entrant behaviour of the resistance, that is the switch in sign of MR as a function of temperature, is dependent on a large magnetic moment at the interface. This result is probably the one which is the easiest to understand. When γ increases the difference in potential experienced by the two different spin species increases and the phases differ more. The z-compent of the magnetic barrier effectively increases or decreases the non-magnetic potential depending on spin of particle and direction of barrier moment. As an example $\gamma = 1$ can give no barrier for spin up particles when $\phi = 0$. With the same parameters the barrier strength will be doubled for spin down particles. If γ is lower the difference will not be that large. With other parameters in the correct range a strong magnetic barrier will then give the best possibility for change of sign in the MR.

The z-component thus raises or lowers the potential, while the y-component introduces an extra phase difference. As for the overall effect of these two components, and thus the complete angle dependence, it is more difficult to give a clear reason for the behaviour without analytical expressions. We will however try to use the difference in coefficients in Fig. 5.6 to give some explanation of the results we have observed. The discussion will then mainly concern the $\gamma = 1$ curves as that is the extreme case.

First we take a look at the $\phi = 0.25\pi$ plots. For low temperatures we see in Fig. 5.2 that there is almost no change in the energy gap. In this region the MR is almost constant negative being dominated by crossed Andreev reflection and direct transmission which at this point together are larger than the positive contribution from normal reflection. When we approach $T = 0.5T_C$ the gap falls faster, and it is at this point we start to see the interesting effects in our plots. Apparently the lowering of the gap will at first enhance the favoring of one alignment for each process. The MR then starts to fall and has a local minima between $T = 0.9T_C$ and $T = 1.0T_C$. It is especially normal transmission and reflection that has had the largest changes. Up to the critical temperature the MR now increases rapidly and eventually becomes positive. The sudden increase for these largest temperatures is caused by the very sudden decrease we have in the energy gap. Crossed Andreev reflection which have given a relatively large negative contribution will then disappear with the energy gap, and direct transmission also gets a smaller magnitude. So even though transmission with spin flip changes sign the normal reflection will dominate more and more and give a positive MR for a temperature around $T = T_C$.

For $\phi = 0.75\pi$ more of the transmission coefficients starts out with a positive dif-

ference between the two alignments, while the opposite is seen for the reflection coefficients. The magnitude of the difference is however smaller. This can be explained by a larger barrier for the spin up particles. For increasing temperatures we find the same trend as for the smaller angle. The magnitude of the difference increases until the MR has an extremal value, which in this case is a maxima. After the maxima both transmission with and without spin flip starts to fall and become negative. Transmission with spin flip follows almost the same curve as for $\phi = 0.25\pi$ and do not seem to be noticeably affected by the change in direction of magnetic moment. Normal transmission on the other hand ends up with a less negative magnitude in this case. And when the normal reflection do not have the small drop it had for $\phi = 0.25\pi$ the MR remains positive even though it falls almost to zero.

These results are for a relatively low value of Z. A change in sign of the MR is however also found for larger barrier potentials, but it seems as if the magnetic potential must be stronger compared to the non-magnetic one. For $Z = 0.35$ we found a sign change for $\gamma = 0.5$, but for $Z = 3.0$ and other parameters the same it seems like a larger γ is needed. It is still at small angles that we find the sign changes. For $\gamma = 0.75$ the MR changes sign for both $\phi = 0$ and $\phi = 0.25\pi$ as we see in Fig. 5.9.

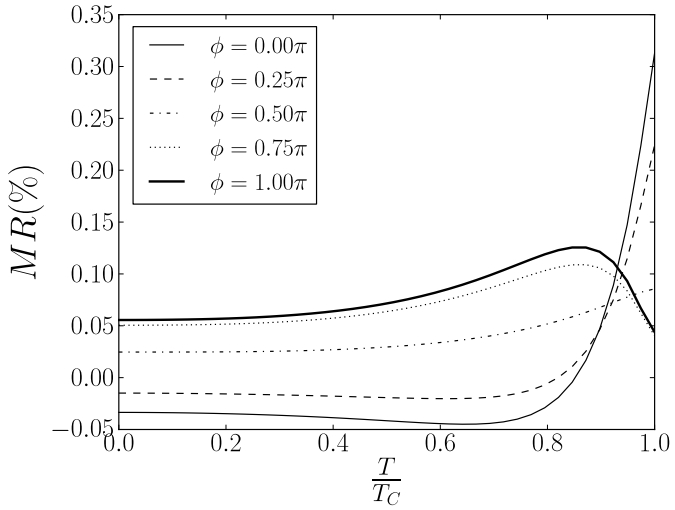

Figure 5.9: The magnetoresistance as a function of temperature for $Z = 3.0$ and $\gamma = 0.75$. The ferromagnets considered have a strength of $x = 0.1$.

As a last comment in this section it is to be said that if we increase the strength of the ferromagnets to $x = 0.5$ a change of sign in MR as a function of T is found also in angles as large as $\phi = \pi$.

5.2.5 Limiting cases

In the previous chapter we found that the regions of full polarization were a geometric effect and would appear even if the superconductor was switched with a normal

metal. It is important to examine if this is the case also for the present structure. In Fig. 5.10 we give a couple of plots with parameters compareable to the one we used in Fig. 5.8. First we see that the curves differ alot from the ones with a superconductor. With a superconductor all curves undergo a rapid increase or decrease as they approached $T = T_C$. Without the superconductor the curves have a slower change. We also find different sign changes of what we previously has observed; the sign changes for $\phi = 0.25\pi$ occur for $T > T_C$, while the sign change for $\phi = 0.75\pi$ is not present in the superconductor plots. It thus seems like it is necessary to include a superconductor to observe the results given in Fig. 5.8.

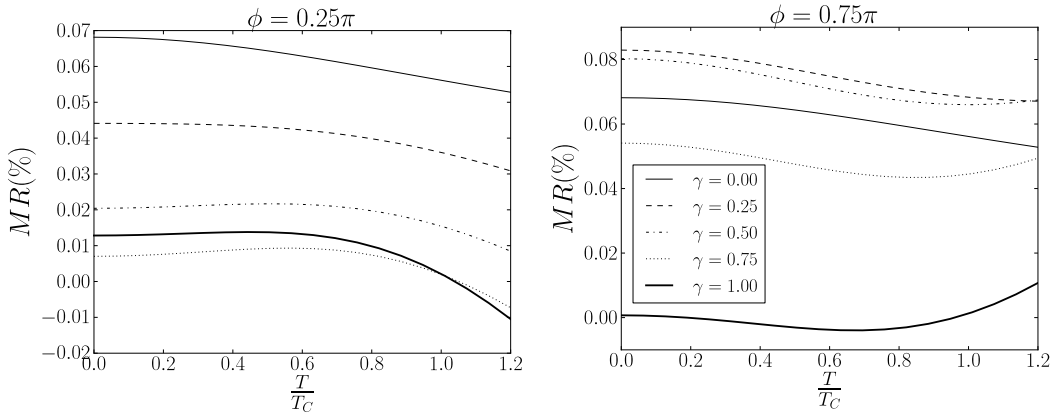

Figure 5.10: The magnetoresistance as a function of temperature for $Z = 0.35$ and different γ and ϕ. The ferromagnets considered have a strength of $x = 0.1$, and the superconductor is switched with a normal metal ($\Delta = 0$).

One last imortant point to mention is the sign of the MR for $\gamma = 0$. In all the plots given we see that in the absence of spin-active interfaces the magnetoresistance is positive for all sets of parameters. This is in line with previous treatments of the F-S-F structure. It would be interesting to know if spin-active interfaces are necessary to get a change in sign of MR. The best would be to find an analytic expression for the MR in the F-S-F structure and then check if this could be negative. Even though it is fairly simple to find analytic expressions for the transmission and reflection coefficients for a simple F-S-F system it is more difficult to find the corresponding general expression for the MR since that involves an energy integration. We can for that reason give no definite conclusion to this question, but our results indicate that it is necessary with spin-active interfaces to observe negative magnetoresistance and the re-entrant effect.

Chapter 6

Conclusion

This thesis has treated the important area of correlations between magnetic and superconducting properties of metals.

We have seen that it is possible to obtain a spin-polarized current from an injected unpolarized current in the N-ZS-N system. A current of nearly 100% spin polarization is obtained in the limit where the normalized barrier strength Z is much larger than 1, that is in the tunneling limit. The interval with full polarization occurs as a consequence of the geometry of the system. At certain energies the probabilities for elastic cotunneling and crossed Andreev reflection have large peaks. These peaks take place at an energy $2h$ less for the spin up current than for the spin down current. In the interval between these two energies the spin up current will dominate and the current will be polarized. A surprising result was obtained when letting Δ go to zero (that is to replace the superconductor with a normal metal) in the analytical and numerical expressions. There were still an area with full polarization. This remarkable result shows that this is mainly a geometrical effect.

The second system examined the possibility to find a re-entrant effect in magnetoresistance as a function of temperature in F-S-F hybrid structures. This effect was recently proved experimentally, and we have looked at spin-active interfaces between the layers as a possible explanation. Our model shows theoretically that this effect can take place in certain parameter ranges. Most important is the strength of the magnetic potential compared with the non-magnetic one. To find a clear re-entrant effect a strong magnetic barrier is needed. This will alter the preferred alignment for some of the transport processes and can, mainly for small angles between the barrier moment and the z-axis, give temperature regions with negative magnetoresistance.

During the last years many steps have been taken in the research of low-temperature spintronics, and it will still be an important field of research for the coming years. The systems considered in this text and other similar and more complex systems will need more theoretical and experimental study. Hopefully this can give new and important insight that can lead to a development in the physical understanding of spin transport, and perhaps new applications.

Bibliography

[1] F. Giazotto and F. Taddei, "Superconductors as spin sources for spintronics," *Phys. Rev. B*, vol. 77, p. 132501, Apr 2008.

[2] M. Colci, K. Sun, N. Shah, S. Vishveshwara, and D. J. Van Harlingen, "Anomalous Polarization-Dependent Transport in Nanoscale Double Barrier Superconductor-Ferromagnet-Superconductor Junctions," *ArXiv e-prints*, Nov. 2011.

[3] J. Bardeen, L. N. Cooper, and J. R. Schrieffer, "Theory of superconductivity," *Phys. Rev.*, vol. 108, pp. 1175–1204, Dec 1957.

[4] J. Bardeen, L. N. Cooper, and J. R. Schrieffer, "Microscopic theory of superconductivity," *Phys. Rev.*, vol. 106, pp. 162–164, Apr 1957.

[5] L. N. Cooper, "Bound electron pairs in a degenerate Fermi gas," *Phys. Rev.*, vol. 104, pp. 1189–1190, Nov 1956.

[6] G. E. Blonder, M. Tinkham, and T. M. Klapwijk, "Transition from metallic to tunneling regimes in superconducting microconstrictions: Excess current, charge imbalance, and supercurrent conversion," *Phys. Rev. B*, vol. 25, pp. 4515–4532, Apr 1982.

[7] A. F. Andreev, "The thermal conductivity of the intermediate state of superconductors," *Sov. Phys. JETP*, vol. 19, pp. 1228–1231, 1964.

[8] M. Eschrig, "Superconductor-metal heterostructures: Coherent conductors at a distance," *Nature Physics*, vol. 5, pp. 384–385, 2009.

[9] A. Knigavko, B. Rosenstein, Y. F. Chen, H. L. Huang, and M. T. Lin, "Ferromagnetic behavior of a triplet superconductor," *Journal of Applied Physics*, vol. 85, no. 8, pp. 6064–6066, 1999.

[10] P. Fulde and R. A. Ferrell, "Superconductivity in a strong spin-exchange field," *Phys. Rev.*, vol. 135, pp. A550–A563, Aug 1964.

[11] A. I. larkin and Y. N. Ovchinnikov, "Nonuniform state of superconductors," *Zh. Eksp. Teor. Fiz.*, vol. 47, pp. 1136–1146, 1964.

[12] K. Fossheim and A. Sudbø, *Superconductivity: physics and applications*. Wiley, 2004.

[13] A. Buzdin, S. Tollis, and J. Cayssol, "Field-induced superconductivity with an enhanced and tunable paramagnetic limit," *Phys. Rev. Lett.*, vol. 95, p. 167003, Oct 2005.

[14] S. Uji and J. S. Brooks, "Magnetic-field-induced superconductivity in organic conductors," *Journal of the Physical Society of Japan*, vol. 75, no. 5, p. 051014, 2006.

[15] A. M. Clogston, "Upper limit for the critical field in hard superconductors," *Phys. Rev. Lett.*, vol. 9, pp. 266–267, Sep 1962.

[16] B. S. Chandrasekhar, "A note on the maximum critical field of high-field superconductors," *Applied Physics Letters*, vol. 1, no. 1, pp. 7–8, 1962.

[17] M. Eschrig, "Spin-polarized supercurrents for spintronics," *Physics Today*, vol. feature article, January, pp. 43–49, 2011.

[18] V. Moshchalkov, R. Woerdenweber, and W. Lang, *Nanoscience and Engineering in Superconductivity*. NanoScience and Technology, Springer, 2010.

[19] M. Hidaka, S. Ishizaka, and J. Sone, "Tunneling of quasiparticles in the normal-insulator-superconductor-insulator-normal geometry," *Journal of Applied Physics*, vol. 74, no. 12, pp. 7402–7409, 1993.

[20] G. Deutscher, "Crossed Andreev reflections," *Journal of Superconductivity*, vol. 15, pp. 43–47, 2002.

[21] C. Nave, "Characteristic lengths in superconductors, http://hyperphysics.phy-astr.gsu.edu/hbase/solids/chrlen.html," May 2012.

[22] J. Linder and A. Sudbø, "Quantum transport in noncentrosymmetric superconductors and thermodynamics of ferromagnetic superconductors," *Phys. Rev. B*, vol. 76, p. 054511, Aug 2007.

[23] P. C. Hemmer, *Kvantemekanikk*. Tapir akademiske forlag, 5th ed., 2005.

[24] J. Cayssol, "Crossed Andreev reflection in a graphene bipolar transistor," *Phys. Rev. Lett.*, vol. 100, p. 147001, Apr 2008.

[25] Z. C. Dong, R. Shen, Z. M. Zheng, D. Y. Xing, and Z. D. Wang, "Coherent quantum transport in ferromagnet/superconductor/ferromagnet structures," *Phys. Rev. B*, vol. 67, p. 134515, Apr 2003.

[26] T. Yamashita, H. Imamura, S. Takahashi, and S. Maekawa, "Andreev reflection in ferromagnet/superconductor/ferromagnet double junction systems," *Phys. Rev. B*, vol. 67, p. 094515, Mar 2003.

[27] J. Linder, T. Yokoyama, Y. Tanaka, and A. Sudbø, "Strongly spin-polarized current generated in a zeeman-split unconventional superconductor," *Phys. Rev. B*, vol. 78, p. 014516, Jul 2008.

[28] S. Das, S. Rao, and A. Saha, "Spintronics with nsn junction of one-dimensional quantum wires: A study of pure spin current and magnetoresistance," *EPL (Europhysics Letters)*, vol. 81, no. 6, p. 67001, 2008.

[29] M. Bozovic and Z. Radovic, "Coherent effects in double-barrier ferromagnet / superconductor / ferromagnet junctions," *arXiv.org:cond-mat*, vol. 0504029v1, Apr 2005.

[30] Q. Zhang, K. S. Chan, and Z. Lin, "Spin current generation by adiabatic pumping in monolayer graphene," *Applied Physics Letters*, vol. 98, no. 3, p. 032106, 2011.

[31] S. Takahashi, H. Imamura, and S. Maekawa, "Spin imbalance and magnetoresistance in ferromagnet/superconductor/ferromagnet double tunnel junctions," *Phys. Rev. Lett.*, vol. 82, pp. 3911–3914, May 1999.

[32] Z. Zheng, D. Y. Xing, G. Sun, and J. Dong, "Andreev reflection effect on spin-polarized transport in ferromagnet/superconductor/ferromagnet double tunnel junctions," *Phys. Rev. B*, vol. 62, pp. 14326–14330, Dec 2000.

[33] M. Johnson, "Spin coupled resistance observed in ferromagnet-superconductor-ferromagnet trilayers," *Applied Physics Letters*, vol. 65, no. 11, pp. 1460–1462, 1994.

[34] L. Lazar, K. Westerholt, H. Zabel, L. R. Tagirov, Y. V. Goryunov, N. N. Garif'yanov, and I. A. Garifullin, "Superconductor/ferromagnet proximity effect in Fe/Pb/Fe trilayers," *Phys. Rev. B*, vol. 61, pp. 3711–3722, Feb 2000.

[35] Y. Obi, M. Ikebe, and H. Fujishiro, "Evidence for zero- and π-phase order parameters of superconducting Nb/Co tri- and pentalayers from the oscillatory behavior of the transition temperature," *Phys. Rev. Lett.*, vol. 94, p. 057008, Feb 2005.

[36] C. Bruder, "Andreev scattering in anisotropic superconductors," *Phys. Rev. B*, vol. 41, pp. 4017–4032, Mar 1990.

[37] J. H. Xu, J. H. Miller, and C. S. Ting, "Magnetic levitation force and penetration depth in type-ii superconductors," *Phys. Rev. B*, vol. 51, pp. 424–434, Jan 1995.

[38] J. Linder, T. Yokoyama, and A. Sudbø, "Spin-transfer torque and magnetoresistance in superconducting spin valves," *Phys. Rev. B*, vol. 79, p. 224504, Jun 2009.